January 1975

An Application of the Utah State University Watershed Simulation Model to the Entiat Experimental Watershed, Washington State

David S. Bowles

J. Paul Riley

George B. Shih

AN APPLICATION OF THE UTAH STATE UNIVERSITY WATERSHED SIMULATION MODEL TO THE ENTIAT EXPERIMENTAL WATERSHED, WASHINGTON STATE

by

David S. Bowles
J. Paul Riley
and
George B. Shih

Prepared for

Forest Service
U.S. Department of Agriculture
Pacific Northwest Forest and Range Experiment Station
Portland, Oregon

Utah Water Research Laboratory
College of Engineering
Utah State University
Logan, Utah 84322

October 1975

PRWG126-1

ABSTRACT

To study the effects of a forest fire on runoff characteristics, the Utah State University Watershed Simulation Model (USUWSM) has been applied to three small drainage areas in the Entiat Experimental Watershed which is located within the Wenatchee National Forest of central Washington. Each component of the USUWSM has been described in the report, including structural changes to the model that were necessary to achieve reasonable agreement between observed and simulated runoff hydrographs. Lack of information on the spatial distribution of precipitation due to the absence of an adequate precipitation gaging network on or close to the study area was a severe handicap to the simulation study. Only a very short period of post-fire streamflow record was available and thus it was possible to make only qualatative conclusions regarding the effects of the forest fire on runoff characteristics.

Keywords: Computer models, Forest-fires, Forest management, Hydrologic models, Mathematical models, Mountain forests, Simulation, Small watersheds, Streamflow, Watershed management, Water yield

ACKNOWLEDGMENTS

This publication represents the final report of a project which was supported primarily with funds provided by the Forest Hydrology Laboratory, Wenatchee, Washington. This laboratory is a part of the Pacific Northwest Forest and Range Experiment Station of the United States Forest Service. The work was accomplished by personnel of the Utah Water Research Laboratory (UWRL) in accordance with a contract which was signed by officials of both Utah State University and the U.S. Forest Service.

Many people assisted with the acquistion of needed data, and provided constructive comments and suggestions throughout the course of this study. Special thanks are extended to Mr. David Helvey of the Forest Hydrology Laboratory in Wenatchee both for the data which he supplied and for his constructive comments and suggestions throughout the course of the entire study, including a careful review of the report manuscript. Gratitude also is expressed to Dr. Richard H. Hawkins and Mr. Eugene K. Israelsen for their constructive reviews of the manuscript.

David S. Bowles
J. Paul Riley
George B. Shih

TABLE OF CONTENTS

LIST OF FIGURES

LIST OF FIGURES (cont.)

LIST OF TABLES

LIST OF PHOTOS

PARTIAL LIST OF SYMBOLS

Symbol	Definition
A	albedo or reflectivity of the snowpack surface
AE	absolute error in prediction of daily runoff for one year
AV	actual evapotranspiration
BF	baseflow
CP(m)	evapotranspiration per ^{o}F of mean monthly temperature for the m^{th} month
D(m)	the number of days in the m^{th} month
EP	potential evapotranspiration
ER	error in prediction of annual streamflow
ET	evapotranspiration
F, F'	freewater depth
f_c	equilibrium infiltration rate
f_o	incremental infiltration rate
G(0)	initial groundwater storage
G(t)	groundwater storage at time, t
G_d	sum of percolation and interflow
G_s	soil moisture above retention capacity
GWR	net withdrawal from the zone of percolation summed over one year
IF	interflow
k_b	proportion of AVSM that becomes baseflow
k''_d	proportion of G_d that becomes interflow
k'_d	value of k''_d approached as $M_s(t)$ approaches M_{cs} from above; dependent on slope and relative magnitudes of vertical and horizontal permability
k_g	decay constant for soil moisture excess treated as a linear reservoir

PARTIAL LIST OF SYMBOLS (cont.)

Symbol	Definition
k_i	proportion of outflow from detention storage which becomes interflow
k_m	snowmelt coefficient
k_s	decay constant from surface runoff and channel precipitation depending upon the basin characteristics (channel precipitation)
k_w	proportion of soil moisture deficit made by withdrawal
LOSS	observed precipitation minus observed streamflow
M_{cs}	soil moisture retention capacity
M_{es}	soil moisture wilting point
M_{rs}	daily snowmelt amount in inches
$M_s(t)$	soil moisture storage
$M_{sn}(t)$	snowpack
M_{ss}	saturated soil moisture storage
n	number of days on which approximate moving average is based
N_r	interflow
P_b	total precipitation at Burns gage for the same period as is used in calculating P_i
P_b'	observed total precipitation at Burns gage for the contemporaneous period
P_i	total precipitation at the i^{th} study area gage for the entire period of observed data at that gage
P_i'	estimated total precipitation at the i^{th} study area gage for the contemporaneous period
PET	potential evapotranspiration
PPT	precipitation
Q_i	observed streamflow on i^{th} day of year
QP_i	predicted streamflow on i^{th} day of year

PARTIAL LIST OF SYMBOLS (cont.)

Symbol	Definition
q	discharge rate from the reservoir
RF	runoff
RH	recharge to zone of percolation
RI	monthly radiation index for the study area
RN	rainfall
S(t)	storage within the basin at any time, t
SDAY	number of days since the last snowfall
S_i	interception storage capacity
$S_i(t)$	interception storage
SM	soil moisture storage
SMMA(t)	approximate moving average of soil moisture storage at time, t
SN	snowfall
SNGM	daily groundmelt from snowpack
SNRF	snow runoff volume
SR	surface runoff
STM	streamflow
T_a	mean daily temperature
TEM	average monthly air temperature
T_m	temperature at which snowmelt commences in ^oF
T_r	temperature above which all precipitation is treated as rain
T_s	temperature below which all precipitation is treated as snow
VR	variance
WD	withdrawal from zone of percolation
WHC	water holding capacity

CHAPTER I

INTRODUCTION

This study was performed for the Pacific Northwest Forest and Range Experiment Station of the United States Forest Service. The objective of the study was to model the hydrologic system of three small drainage areas in the Entiat Experimental Watershed in order to help understand effects on runoff characteristics resulting from management and other changes in the watershed. In particular, the ability of the model to predict these effects is demonstrated by simulating runoff hydrographs associated with pre-fire and post-fire conditions on the watershed.

When the experimental watersheds were first established, the Forest Service planned to investigate the effects of various management practices on streamflow. Two of the three watersheds were to have been subjected to various management practices while the third was to be left in its natural condition to act as a "control" area. Streamflow correlation relationships were established between the control watershed and each of the other two watersheds. As management practices were applied to the first two watersheds, the measured streamflow quantities were compared with the estimate of streamflows that would have occurred in the absence of management, the estimated quantities being obtained from the correlation relationships with the third watershed. In this way, changes in streamflows associated with particular management practices were estimated. However, on August 24, 1970, an uncontrolled forest fire swept across parts of the experimental watersheds, including the control area, and thus changed the emphasis of the study to one of investigating the effects of forest fires on streamflow.

Because the forest fire changed vegetation conditions on each of the three study areas, it no longer was possible to use the control watershed to predict runoff from the other two areas under virgin conditions. For this reason, hydrologic simulation was proposed as a technique for predicting the effect of the fire on the runoff characteristics of each of the three study areas. In addition, it was considered that the development and application of a hydrologic simulation model would provide increased insight into (1) the basic hydrologic processes occurring within the study areas, and (2) additional data requirements to support further investigations.

To form a watershed hydrologic simulation model a collection of mathematical submodels, each representing basic physical processes in the hydrologic cycle (see Figure 1), are linked together by applying the concept of continuity of mass. This synthesis of the mathematical submodels into a dynamic model of the prototype system is achieved with the aid of a digital computer. The model transforms measured or estimated meteorologic inputs into predicted outflow functions from the watershed. When the model adequately represents the prototype system, the computed outflow closely resembles the observed outflow. Thus, the comparison between computed and observed streamflow provides a check on the adequacy of the model. Furthermore, the model can be applied to any other watershed containing the same major hydrologic processes by adjusting the model parameters to reflect the new watershed characteristics.

In this study the model was verified (calibrated and tested) using eight years of pre-fire data. During the verification stage, the model components were tested and improved to define the system as accurately as possible. The model then was run to represent the one year of post-fire conditions for which data were available. This run was accomplished by changing several of the model parameters to appropriate values based on observed post-fire conditions. When the same set of meteorological data were input to the model using firstly the pre-fire parameter set, and secondly the post-fire parameter set, the differences between the computed streamflow for these two runs provided an estimate of the effects of the forest fire on streamflow characteristics.

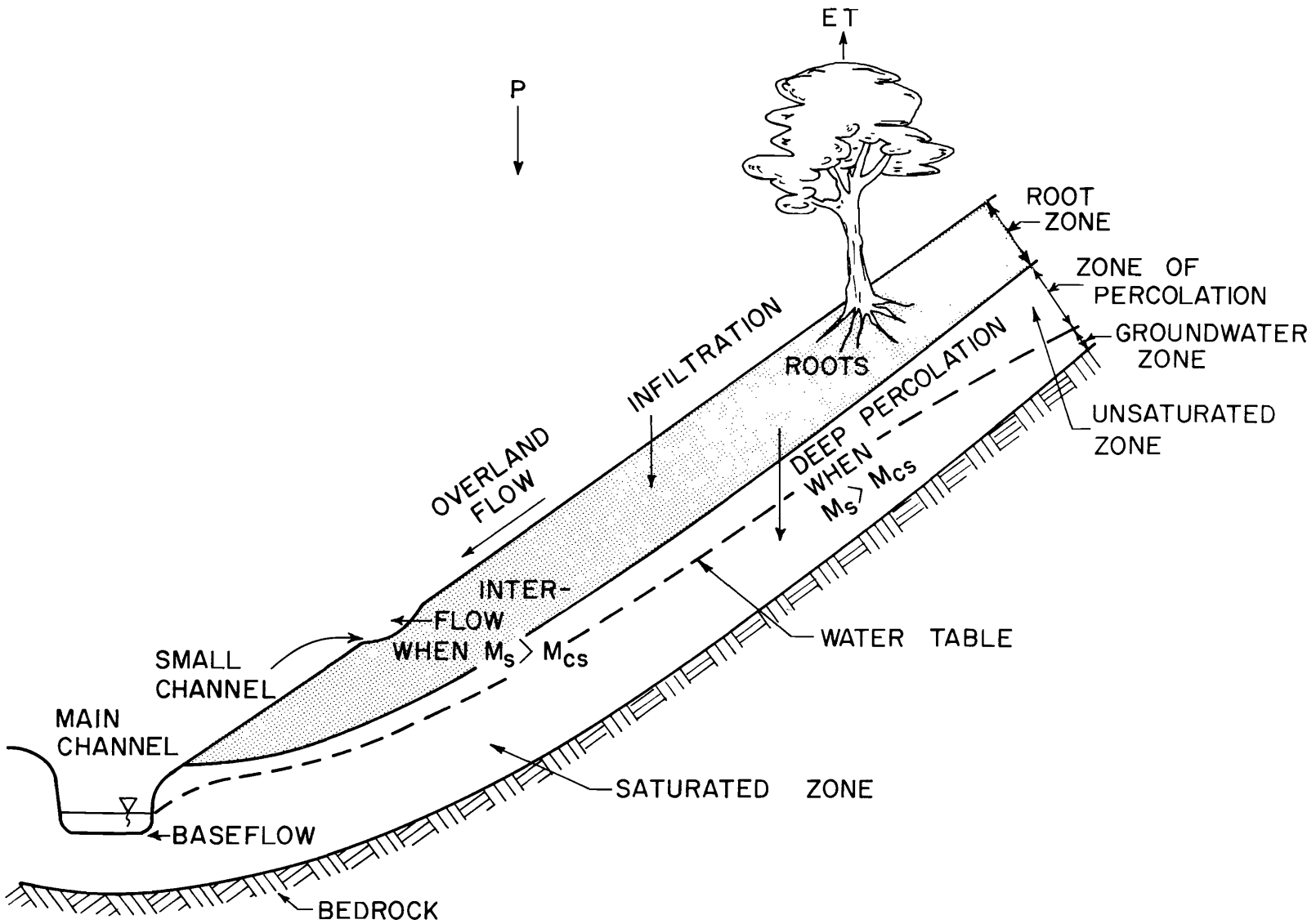

Figure 1. The terrestrial part of the hydrologic cycle in a steep mountain watershed as represented by original Utah State University Watershed Simulation Model (USUWSM).

CHAPTER II

THE STUDY AREA

The Entiat Experimental Watershed is located about 50 miles (80 km) north of Wenatchee and is part of the Wenatchee National Forest in Washington State (see Figure 2 and Photos 1 and 2). The Entiat Experimental Watershed was set aside in 1957 as a study area representative of much of the forested lands east of the Washington Cascade Mountain creast (Berndt, 1967).

Three adjacent drainage areas within the experimental forest were simulated in this study. Each area is a hanging valley formed by glacial action and oriented in a general southwest direction between Four-mile Ridge, the northern watershed boundary, and the Entiat River (see Figure 2). The streams which drain these three areas are Fox, Burns, and McCree Creeks. Each watershed is approximately two square miles (3,200 ha) in area with elevations ranging from 2,000 feet (609.6 m) to 7,100 feet (2,164 m) and a mean slope of about 50 percent, but slopes as steep as 90 percent are common.

Klock (1971) describes the soils of the area as follows:

> The base rock on the watersheds is an extensive formation known as the Chelan Batholith, a mesozoic intrusive granodiorite with biotite and hornblende as accessory minerals. A medium- a coarse-grained massive rock, the gray granodiorite weathers deeply where exposed. Since glaciation, the area has been periodically covered by volcanic ash and pumice, mostly originating from Glacier Peak (Fryxell, 1965) approximately 33 kilometers (21 miles) west-northwest of the study area.

The Choral soil series occupies about 55 percent of the area (Iritani and Meyer, 1967). Rampart soils occupy another 30 percent, and rock land or rock outcrops account for 15 percent. Choral soils are well drained, moderately coarse

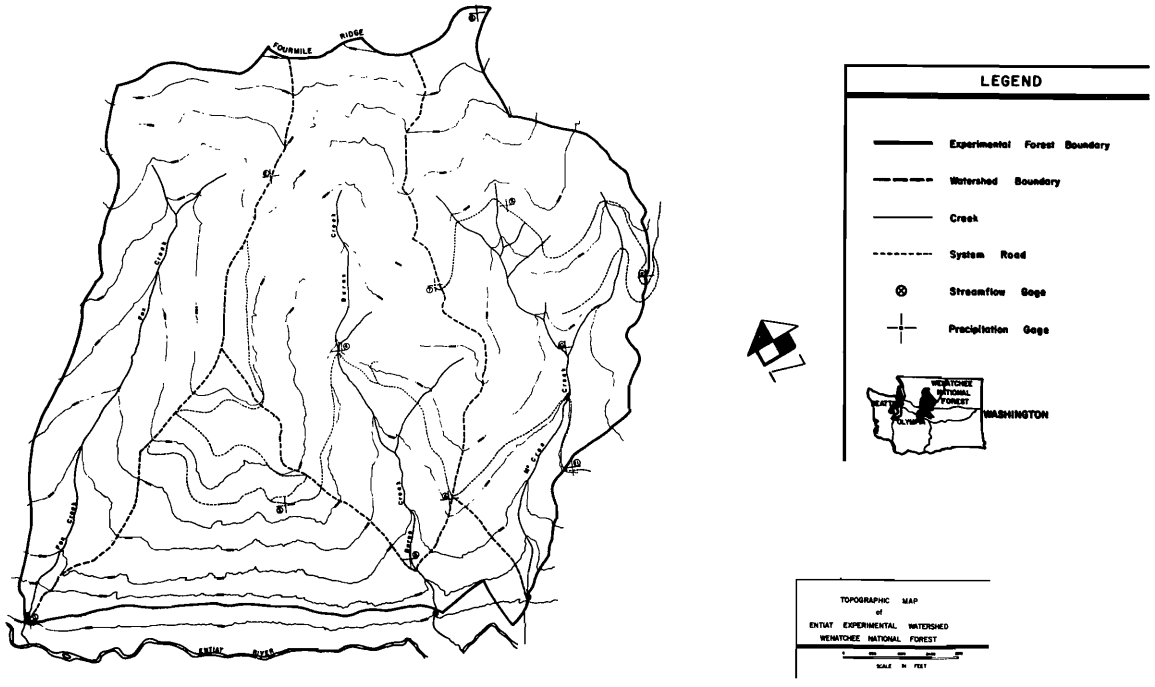

Figure 2. Topographical map of the three study watersheds in the Entiat Experimental Watershed (1 ft. = 0.305 m).

Photo 1. View of burnt study area.

Photo 2. View of burnt study area.

textured, and derived from volcanic ash and pumice. The surface 60 centimeters (24 ins.) is a fine, sandy loam grading to coarse, loamy sand. This is underlain by pure pumice up to 6 meters (20 ft.) deep. Rampart soils are very similar to Choral except they occur at lower elevations and have developed under warmer climatic conditions.

Pre-fire vegetation also is described by Klock (1970):

> Vegetation destroyed by the fire was almost entirely mature virgin forest. Ponderosa pine (Pinus ponderosa Laws.) was the main species with Douglas-fir (Pseudotsuga menziesii (Mirb.) Franco) as the main associated species. Stocking densities ranged from medium to poor. Common understory species were snowbrush ceanothus (Ceanothus velutinus Dougl.), bitterbrush (Purshia tridentata (Pursh)DC.), grouse whortleberry (Vaccinium scoparium Leib.), and pinegrass (Calamagrostis rubescens Buckl.).

Average annual precipitation for the entire study area was estimated to be about 28 inches (710 mm). Typically, about two-thirds of the annual precipitation is in the form of snow. With the exception of snowmelt flows, pre-fire streamflow remained remarkably uniform and was not very responsive to rainfall. This unresponsiveness of streamflow volumes to precipitation volumes is demonstrated at the annual level by Figures 3, 4, and 5. For example, 1970 annual streamflow is only slightly different from 1963 annual streamflow, but 1963 annual precipitation is approximately four times the 1970 annual precipitation. The 1971 points on Figures 3, 4, and 5 represent the first year after the destruction of vegetation by wildfire, and demonstrate an increased responsiveness after the fire. At the daily level the unresponsiveness of observed streamflow to individual precipitation events can be observed from Figure 19.

Helvey (1973) has suggested that the streams are not very responsive to rainfall because summer storms are not large enough to satisfy moisture deficits in the soil water or rooting zone. Mean annual flows for the Fox, Burns, and McCree Creeks during the study period were 7.11 inches (181 mm), 6.08 inches (154 mm), and 4.27 inches (108 mm), respectively. Freezing temperatures persist for 5 months of each year. The annual mean temperature over the entire study area was estimated to be about 40°F (4.4°C).

The forest fire resulted from an intense dry lightening storm that swept across much of north-central Washington State during the early morning hours of August 24, 1975. Berndt (1971) describes the fire as "one of the most serious fire disasters ever to occur in the region. Ultimately, about 115,000 acres (284,000 ha) of timber were devastated in this single lightening-fire sequence. This area included the Entiat Experimental Forest where water yeilds, climate, and other environmental variables" had been studied for nearly 10 years on the three small watersheds.

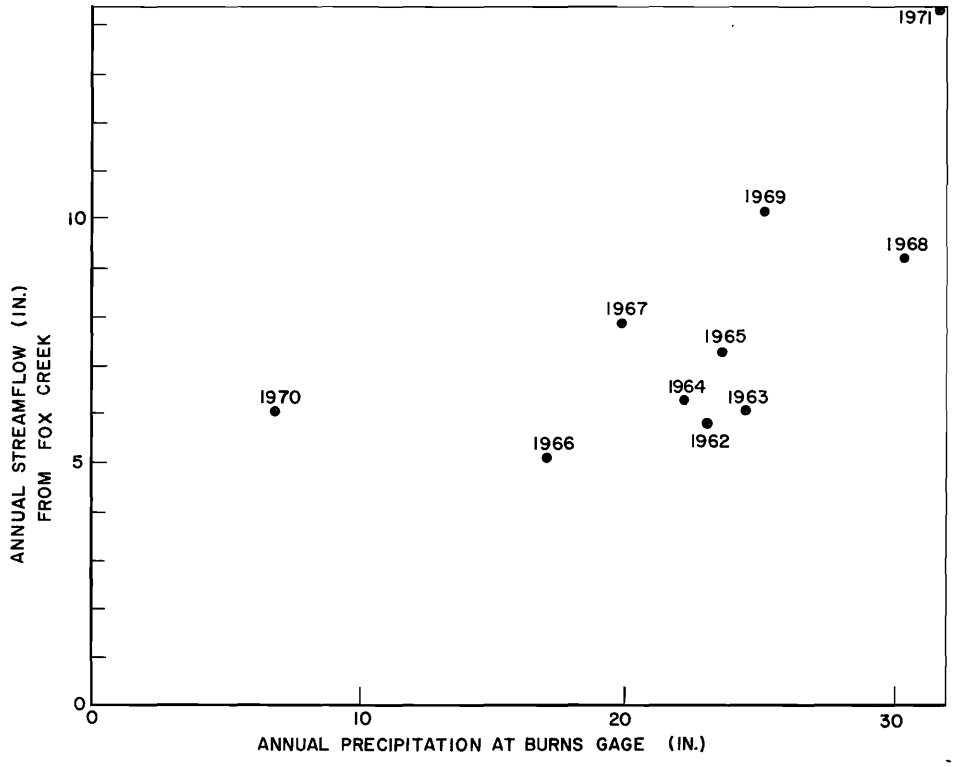

Figure 3. Annual streamflow from Fox Creek versus annual precipitation at Burns gage (1 in. = 25.4 mm).

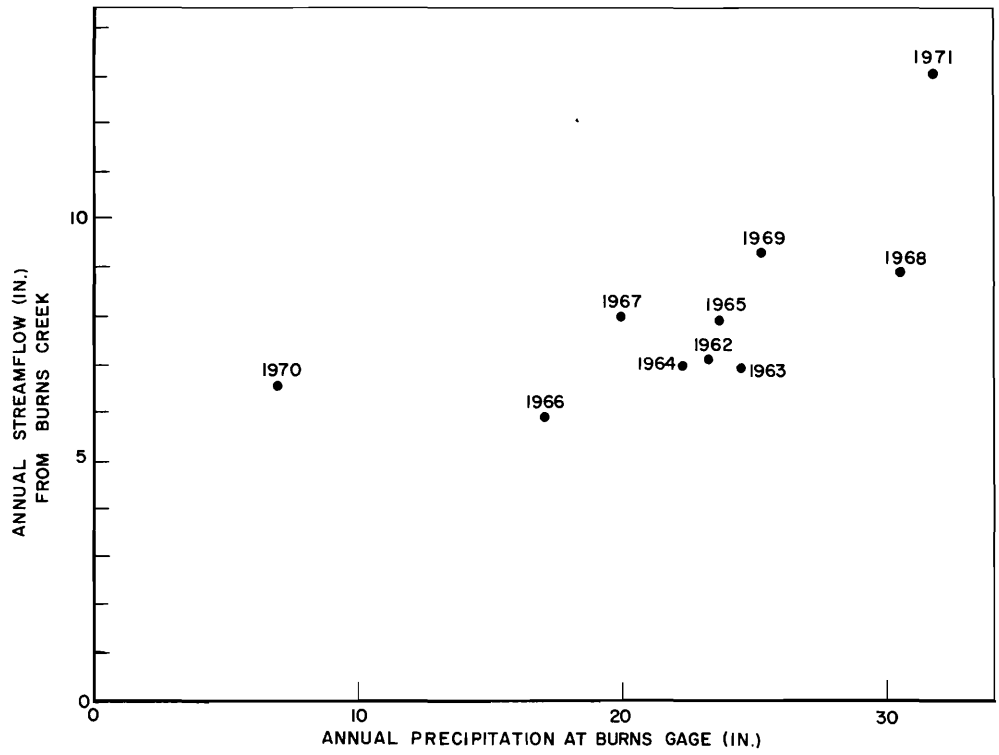

Figure 4. Annual streamflow from Burns Creek versus annual precipitation at Burn gage (1 in. = 25.4 mm).

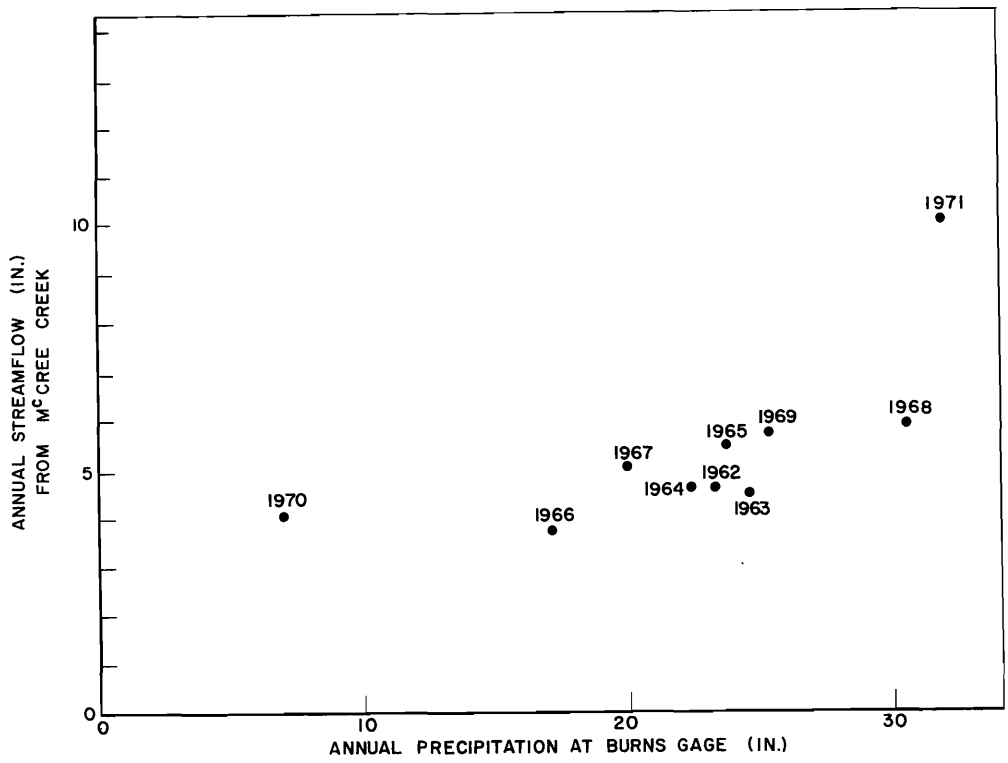

Figure 5. Annual streamflow from McCree Creek versus annual precipitation at Burns gage (1 in. = 25.4 mm).

CHAPTER III

DATA PREPARATION

The time increment for the Utah State University Watershed Simulation Model (USUWSM) is one day, and therefore daily data are required. Daily streamflow, precipitation, and temperature data were supplied by the U.S. Forest Service. Separate data were prepared for each of the three watersheds for a study period of nine years duration commencing on October 1, 1962. The preparation of each type of data is briefly described below.

Streamflow

Daily streamflow data in cubic feet per second were supplied on punched cards. These data for each watershed were converted from cubic feet per second to inches since USUWSM is written to accept streamflow data in inches.

Precipitation

There is only one precipitation gage in the study area with records covering the entire study period. This gage is located close to the downstream extremity of the Burns watershed. Runoff yield per unit area was computed for each watershed and the values obtained showed marked differences between watersheds. If it is assumed that pre-fire evapotranspiration characteristics for the three watersheds were fairly homogeneous, and that no important subsurface flows exist across the watershed boundaries, then the differences between the runoff ratios are due to differences in the amount of precipitation on each area. Following this reasoning, a basis was sought for the spatial distribution over the study area of precipitation measured at the single precipitation gage.

Precipitation records were available for two sets of gages. The first, which covered the complete study period, was comprised of the Burns station and six other stations on an approximate radius of 30 miles (48 km) from the experimental watershed (see Figure 6). The second data set consisted of nine stations situated on the study area (see Figure 2). These records were available for varying periods, each of approximately one year in length. Precipitation records at each of these study area gages were extended to provide nine contemporaneous records. The extension of these precipitation records was accomplished by the following weighting procedure based on the precipitation record at the Burns gage:

$$P_i' = \frac{P_i}{P_b} P_b' \quad \ldots\ldots\ldots \quad (1)$$

in which

P_i' = estimated total precipitation at the i^{th} study area gage for the contemporaneous period

P_b' = observed total precipitation at Burns gage for the contemporaneous period

P_i = total precipitation at the i^{th} study area gage for the entire period of observed data at that gage

P_b = total precipitation at Burns gage for the same period as is used in calculating P_i

To establish a criterion for obtaining the different precipitation amounts on each watershed, a multiple linear regression was performed for each data set. Mean annual precipitation was correlated with station elevation and east-west distance of the station from an arbitrary datum. The first data set provided the highest coefficient of correlation (R^2) with a value of 0.89.

The regression equation (see Figures 7 and 8) is given as follows:

$$P = 40.127 - 0.995 \text{ (Distance east of Steven's Pass)} + 0.007 \text{ (Elevation)} \quad \ldots\ldots\ldots \quad (2)$$

Equation 2 was used to estimate mean annual precipitation (P) for a watershed based on its mean elevation and the distance east from Steven's Pass to the watershed's centroid of area. Daily precipitation for a watershed then was obtained by multiplying the corresponding daily precipitation measured at the Burns gage by the ratio of estimated mean annual precipitation for the watershed, to the mean annual precipitation at the Burns gage. It is emphasized that the regression equation used was obtained using data from stations located approximately 30 miles (48 km) from the study area.

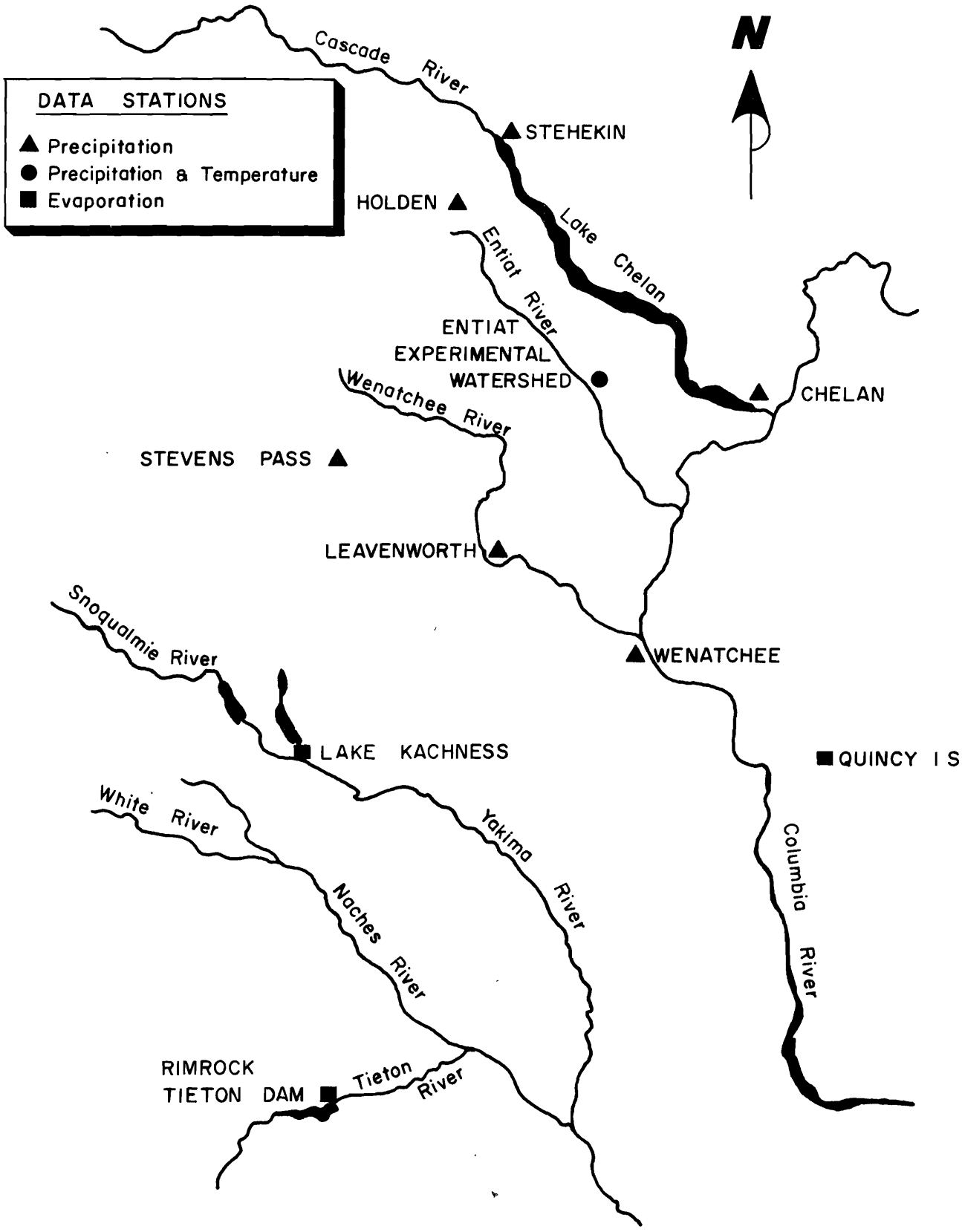

Figure 6. Map showing location of data stations.

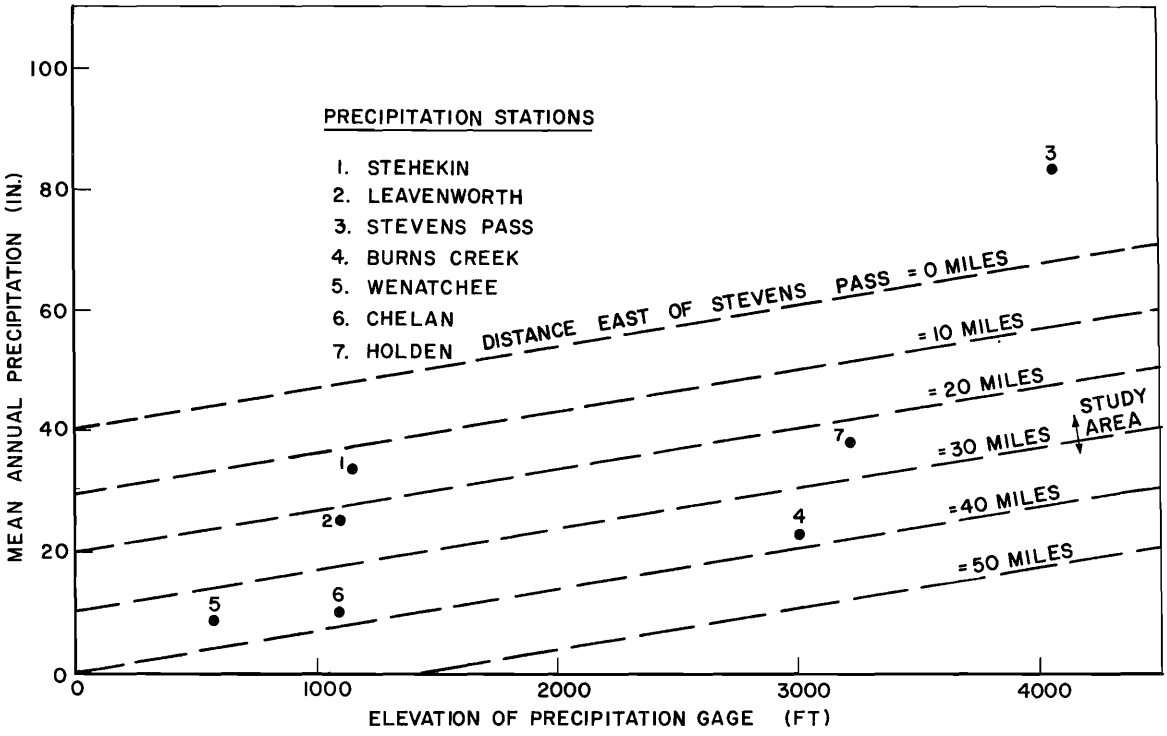

Figure 7. Mean annual precipitation versus precipitation gage elevation as a function of distance east of Steven's Pass for the set of precipitation stations approximately thirty miles from study area (1 in. = 25.4 mm, 1 ft. = 0.305 m, 1 mile = 1.61 km).

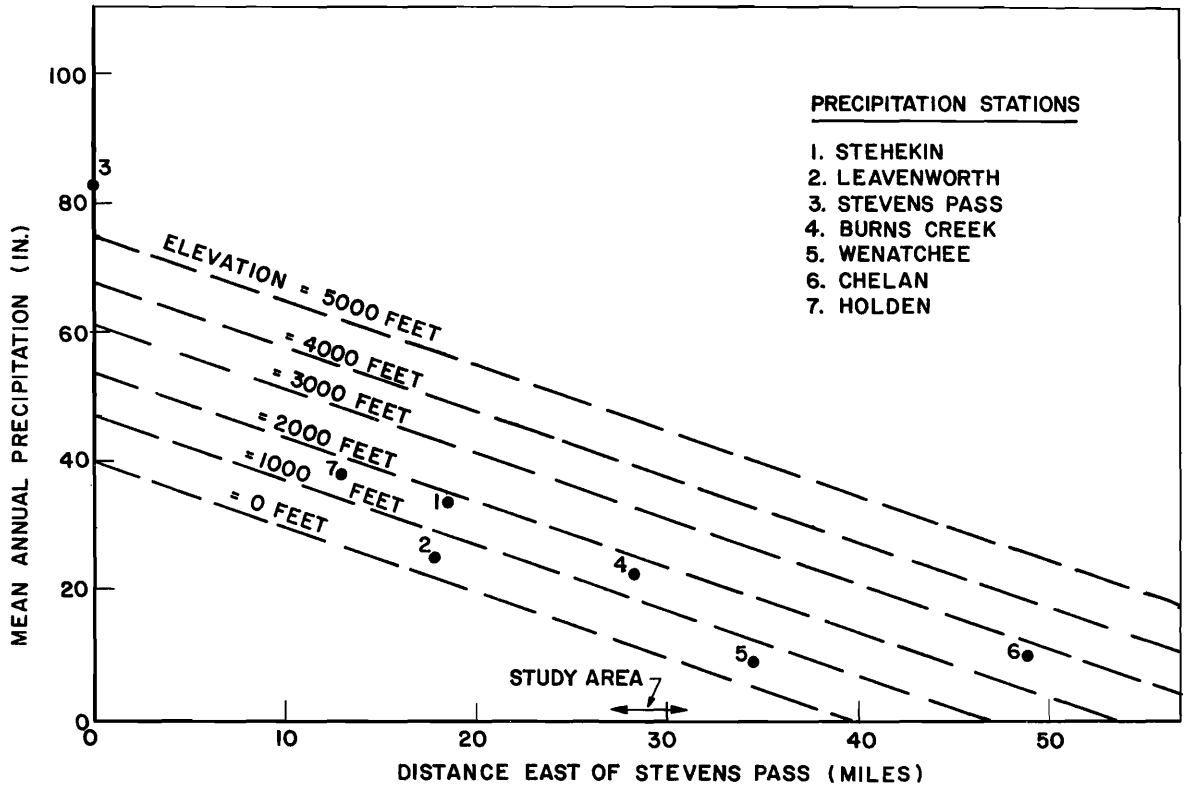

Figure 8. Mean annual precipitation versus distance east of Steven's Pass as a function of precipitation gage elevation for the set of precipitation stations approximately thirty miles from study area (1 in. = 25.4 mm, 1 ft. = 0.305 m, 1 mile = 1.61 km).

Temperature

The daily temperature at the Burns station was lapsed to the mean elevation of each watershed. Monthly lapse rates were estimated by linear regression using lapse rates available for Spokane, Washington. The data were obtained from Climatological Data by the U.S. Department of Commerce (1961 through 1970).

Evapotranspiration

Monthly pan evaporation and mean monthly temperature data were obtained from Climatological Data (1961 through 1970) for 10 years of record at Quincy 1S and Rimrock Tieton Dam. Records at Lake Kachness, an evaporation station closer to the study area than Rimrock Tieton Dam, were not available for the complete study period. Mean monthly amounts of evaporation, per ^{o}F of mean monthly temperature, were computed for both stations and the mean of these two values was used for the study area. This value was divided by the number of days in the month and multiplied by the temperature of a particular day to obtain an estimated potential evapotranspiration rate for that day. This approach for estimating potential evapotranspiration was adopted by Shih et al. (1972) in an earlier version of USUWSM.

Solar radiation

At a particular location on the earth's surface the direction and degree of slope strongly influence the amount of direct solar radiation which is received on that slope. Thus, for a north-facing slope evapotranspiration and snowmelt rates tends to be lower than is the case for a south slope. For this reason, in the watershed hydrology model which is used an attempt is made to account for the average degree of slope and direction (aspect) of the area under study. The parameter which is applied is termed the solar radiation index (Lee, 1963; Riley et al., 1966). This index is a relative measure of the amount of direct solar radiation received by a given slope at a particular location and time to that received by a horizontal surface at the same location and time. Because the effects of atmospheric conditions are assumed to be the same for both surfaces in the same location, atmospheric effects are assumed to be removed. Monthly radiation index values for each watershed were determined as a function of aspect, percent slope, and time of year. Because the average slope, aspect, and latitude are essentially the same for each of the three watersheds, the same monthly radiation index value was applied to each area. These values are shown by Table 1 which appears later in the report in Chapter V.

CHAPTER IV

THE UTAH STATE UNIVERSITY WATERSHED SIMULATION MODEL

The basic model used in this project is termed the Utah State University Watershed Simulation Model (USUWSM), and was first developed by Riley et al. (1966). Shih (1971) extended this work in a study of water budgeting and weather modification for the Weber River Basin, Utah. The model was further modified by Shih et al. (1972) and was successfully applied to a watershed in the H.J. Andrews Experimental Forest for the Coniferous Forest Biome (Chambers, 1973). In addition, the model was applied to the Olympus Cove area, Salt Lake County, Utah (Riley et al., 1974) in a hydrologic study of an urbanizing watershed. The model is currently being used in a bio-hydrologic study of Spawn Creek, near Logan, Utah (Twedt, 1975).

USUWSM is a lumped parameter model with a time increment of one day. Some changes and refinements were made to the model during the study to account for characteristics of the prototype relating to the unresponsiveness of streamflow to rainfall and the importance of snow. Figure 9 is a simplified flow chart of the hydrologic system represented by the model. A listing of the FORTRAN computer program is contained in the Appendix. Brief descriptions of each component of the model are given by the following paragraphs.

Interception

Interception is that part of precipitation which is temporarily held by forest canopies and then returned to the atmosphere by evapotranspiration or sublimation. The amount of interception depends on storm size and intensity, and canopy type and density. For each storm the available interception storage capacity of the canopy must be satisfied before precipitation is assumed to reach the ground surface. Hence the potential amount of interception abstraction at any time is given by $S_i - S_i(t)$ where S_i is the maximum interception storage capacity of the canopy and $S_i(t)$ is the interception storage occupied at time t. For the study areas, the average value of S_i was determined through the calibration procedure to be 0.2 inches (5 mm). Because evaporation had depleted previous interception storage quantities, for most storms the initial value of $S_i(t)$ was zero.

Snow accumulation and ablation

Figure 10 is a flow chart of the snow accumulation and ablation processes. The following temperature criterion is used to divide the daily precipitation (P) into rain (R) and snow (S) (Figure 11):

$$SN = P\,\frac{T_r - T_a}{T_r - T_s} \quad , T_s < T_a < T_r \quad . \quad . \quad (3a)$$

$$SN = 0 \quad , T_a \geq T_r \quad . \quad . \quad . \quad (3b)$$

$$SN = P \quad , T_a \leq T_s \quad . \quad . \quad . \quad (3c)$$

$$R = P - SN \quad , \text{for all } T_a \quad . \quad . \quad (3d)$$

in which T_a is the mean daily temperature; T_r is the temperature above which all precipitation is treated as rain; and T_s is the temperature below which all precipitation is treated as snow. The above relationship is drawn from earlier work by the U.S. Army Corps of Engineers (1956). The values determined during the calibration process for T_r and T_s were 38°F (3.3° C) and 30° F (-1.1°C) respectively.

Snowmelt rate depends primarily upon the rate of energy input to the snowpack. However, the complex nature of the process and the scarcity of relevant data prevent a strictly analytical approach to the simulation of snowmelt. Air temperatures are frequently used as an index of available energy (Pysklywec et al., 1968; Anderson and Crawford, 1964; Amorocho and Espildora, 1966; and Eggleston et al., 1971).

A degree day approach shown in Equation 4 and based on the work of Eggleston et al. (1971) was used to represent the snowmelt process at the surface of the snowpack. Equation 4 consists of two terms, a radiation melt term and a rain on snowmelt term.

$$M_{sr} = \overbrace{k_m R I\,(T_e - T_m)(1 - A)}^{\text{radiation}} + \overbrace{(T_a - 32)\,\frac{R}{144}}^{\text{rain on snow}} \quad . \quad . \quad (4)$$

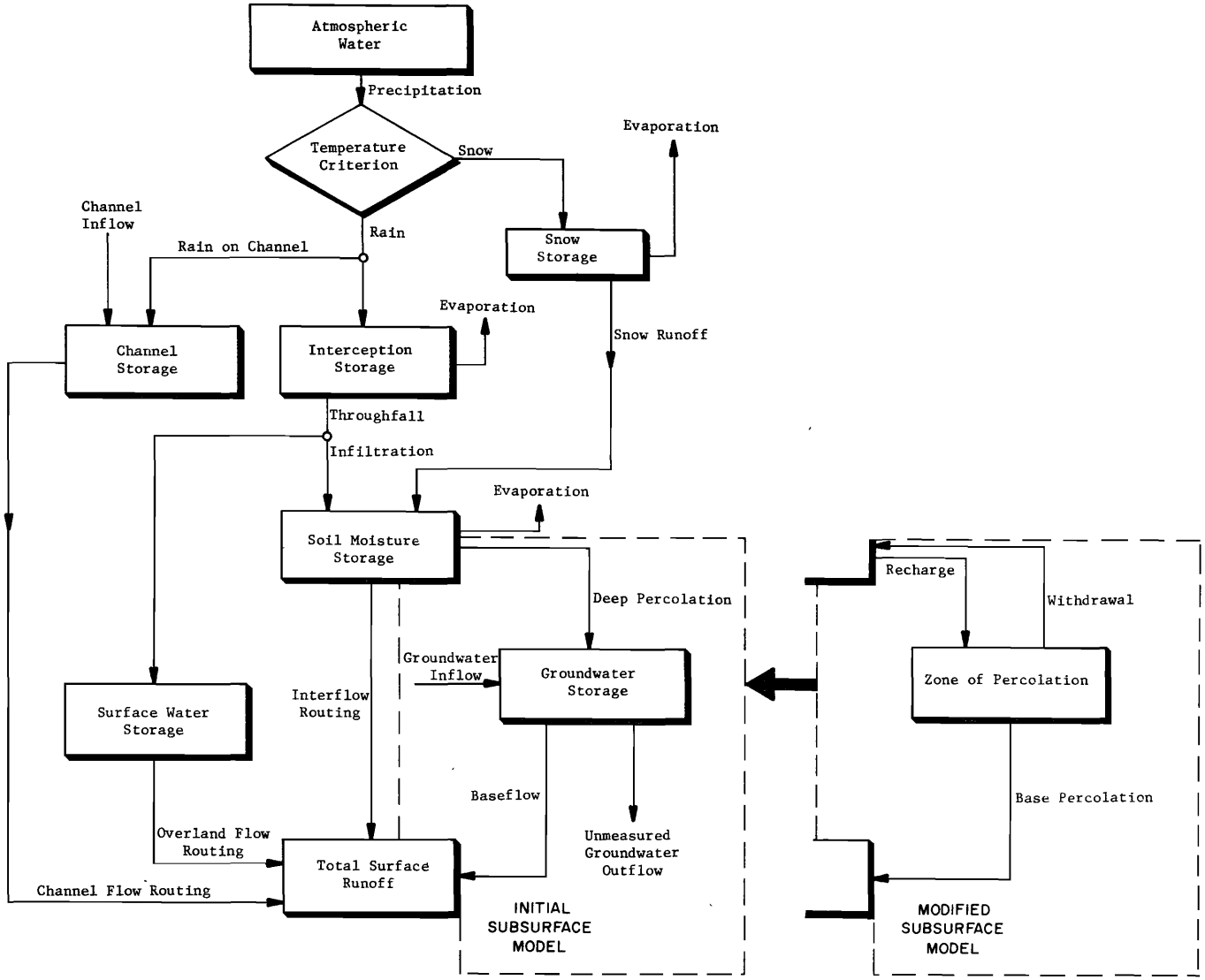

Figure 9. Simplified flow chart of the hydrologic system represented by USUWSM.

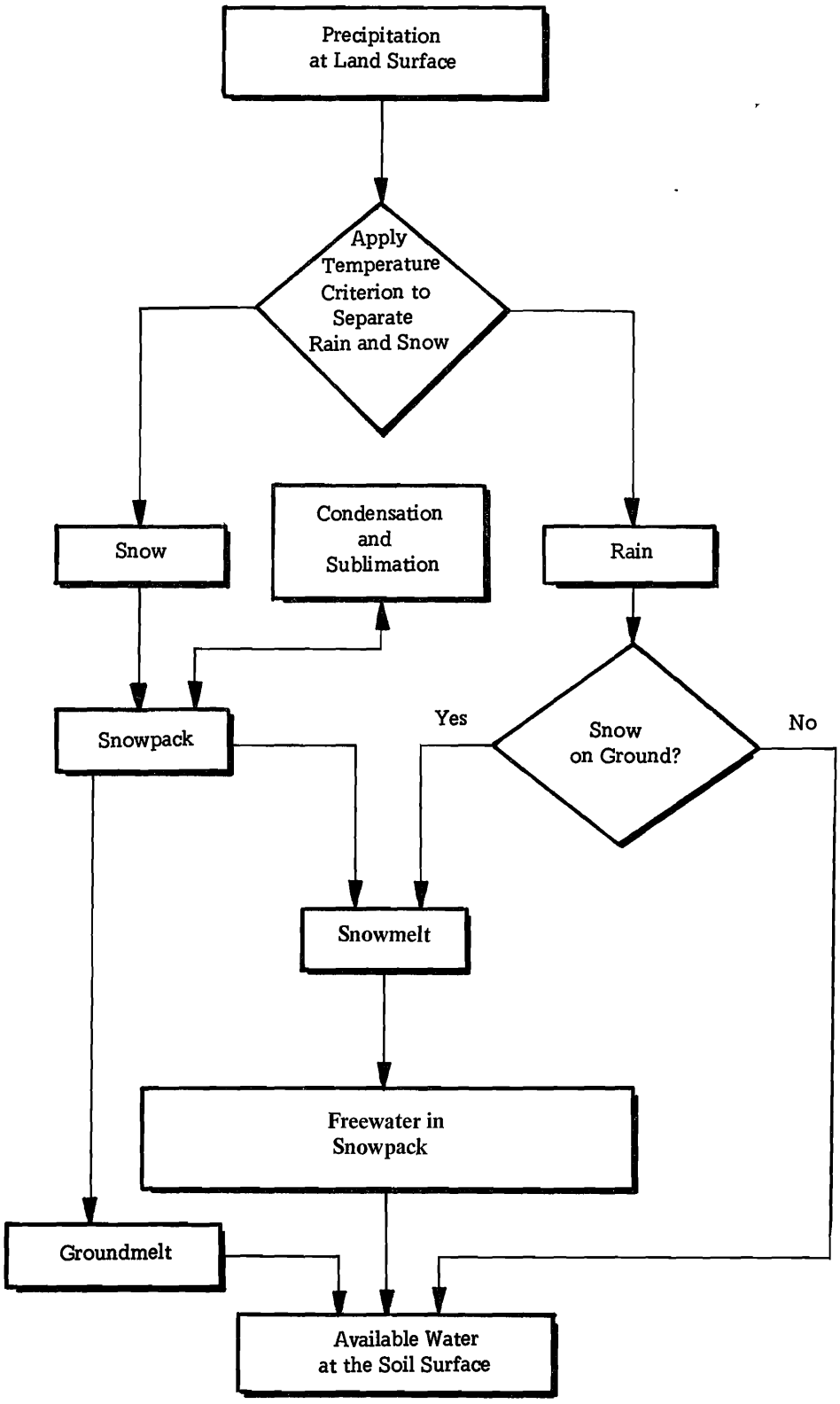

Figure 10. Flow chart of the snow accumulation and ablation processes represented by USUWSM.

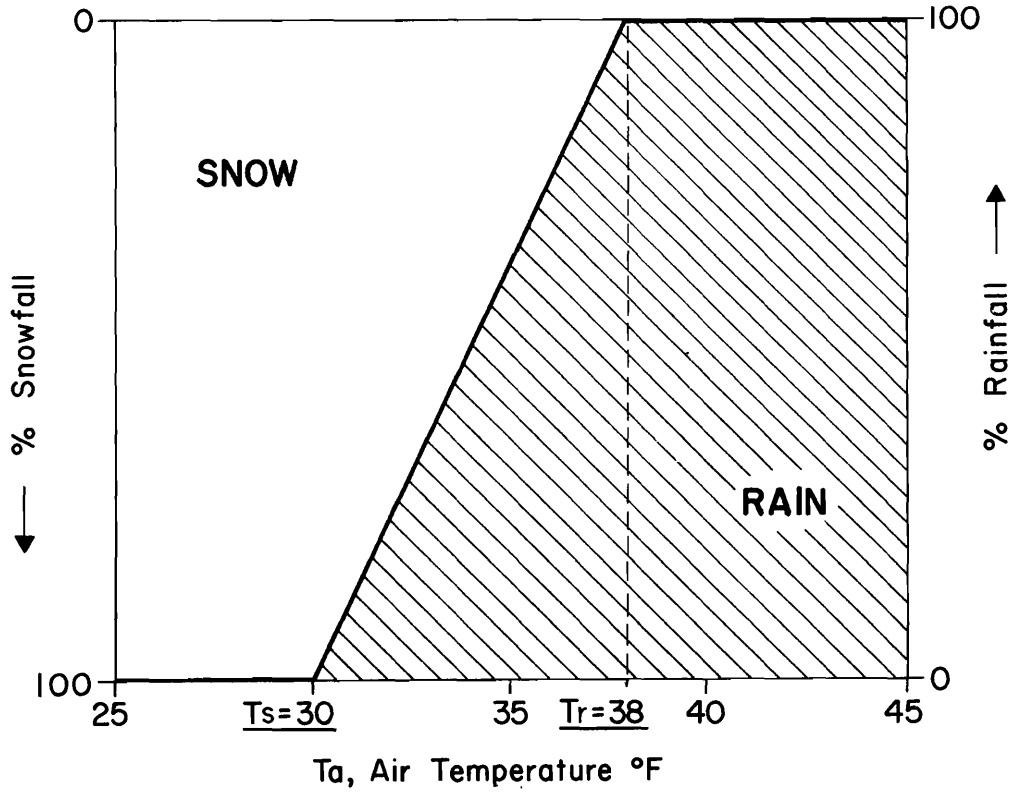

Figure 11. Temperature criterion used to divide daily precipitation into rain and snow (^{o} F = 9/5 ^{o}C + 32).

in which M_{rs} is the daily snowmelt amount in inches; k_m is the snowmelt coefficient; RI is the monthly radiation index for the study area; T_a is the mean daily air temperature in ^{o}F; T_e is the snowpack temperature in ^{o}F; T_m is the temperature at which snowmelt commences in ^{o}F; R is the rainfall in inches, and A is the albedo or reflectivity of the snowpack surface.

Albedo is calculated in the following manner:

$$A = 0.4\,(1 + e^{-0.2\,SDAY}) \quad , R = 0 \quad . \; . \; (5a)$$

$$A = 0.4 \quad , R > 0 \quad . \; . \; (5b)$$

in which SDAY is the number of days since the last snowfall. Thus, albedo decreases during periods without fresh snow and reaches a lower limit of 0.4 when rainfall occurs.

Freewater in the snowpack comprises snowmelt and rain that has fallen onto the snowpack (see Figure 10). The freewater either freezes within the snowpack or emerges from the bottom of the pack after its liquid water holding capacity is satisified and enters the soil moisture zone. There also exists a possibility of evaporation of freewater which is considered later in the description of the evaporation component of the model. In the study area the large change in elevation and consequent change in air temperatures results in a variation of snowmelt and therefore depth of freewater over the watershed. Runoff from the snowpack will occur when the depth of freewater (F) exceeds the liquid water holding capacity (WHC) of the snowpack. In the prototype system the situation of freewater depths exceeding the water holding capacity occurs earlier in the snowmelt season at lower elevations than at higher elevations. Thus, snow runoff takes place at lower elevations before higher elevations. However, the lumped parameter model simulates snow runoff over the entire watershed area when the depth of freewater at the mean elevation exceeds the water holding capacity of the snowpack.

The dependency of the lumped parameter model on the freewater status at only the mean elevation results in a significant discrepancy in the timing of snow runoff for the study area in which large elevation

changes are present. For example, on some days actual snow runoff will occur from lower elevations before it occurs at the mean elevation. On these days simulated runoff was zero because F < WHC at the mean elevation and therefore the actual snow runoff from the lower elevations was not simulated. Another example is the situation in which actual snow runoff occurs at the mean elevation but not at higher elevations. Under these conditions the simulated snow runoff volume was equal to the depth of snow runoff (F - WHC) multiplied by the entire watershed area including the higher elevations where no snow runoff actually occurred.

To improve the timing of snow runoff it was necessary to introduce a method of accounting for the variation in F, the freewater depth over the different elevation ranges in the watershed area. The distributed parameter approach in which each watershed is divided into several spatial units based on elevation intervals was ruled out by the lack of sufficient data. A procedure was devised in which spatial resolution of the lumped parameter model was improved without resorting to reduced spatial units. It was assumed that there existed a linear variation in freewater depth (F') over the watershed area. Figure 12 shows three cases that may arise:

Case I: Freewater depth (F') over part of the watershed is less than WHC and over the remainder of the watershed is above WHC. In this case, only that part of the watershed area in which F' > WHC contributes to snow runoff. The amount of snow runoff is found by calculating the cross-hatched area between F' and WHC when F' > WHC. By simple geometry it can be shown that the volume of snow runoff is:

$$SNRF = \frac{(F + S/2 - WHC)^2}{2S} \quad . \; . \; . \quad (6)$$

Case II: Freewater depth (F') is greater than WHC over the entire watershed. Snow runoff takes place over the total watershed area. The volume of snow runoff is:

$$SNRF = F - WHC \; . \; . \; . \; . \; . \; . \; . \quad (7)$$

Case III: Freewater depth (F') is less than WHC over the entire watershed and therefore no snow runoff occurs:

$$SNRF = 0 \; . \; . \; . \; . \; . \; . \; . \; . \; . \quad (8)$$

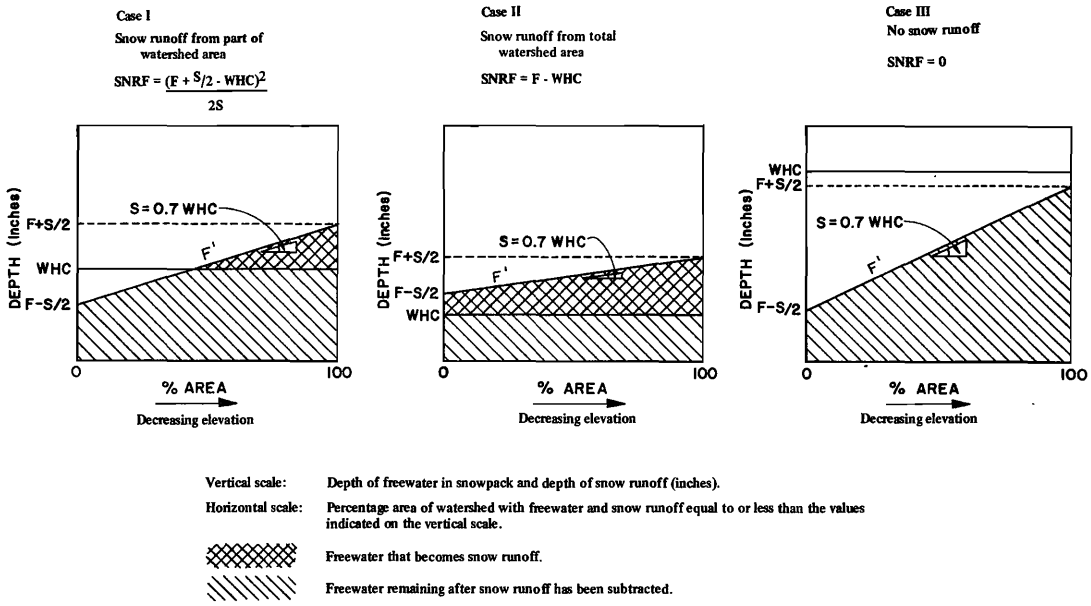

Figure 12. Three cases illustrating the method of estimating snow runoff (1 in. = 25.4 mm).

The cross-hatched areas of Figure 12 represent the volume of snowmelt runoff, while the shaded areas represent the volume of freewater remaining after snow runoff, has been subtracted. Vertical axes represent depths of freewater and snow runoff and horizontal axes represent percent watershed area. The choice of percent watershed area for the horizontal axes results in the snow runoff volume SNRF being expressed as an equivalent depth in inches over the entire watershed area. In this way, SNRF is compatible with the other variables in the model which also are stored as depths in inches.

Previous versions of the snow model did not include any consideration of variation in snow runoff at different locations in the watershed and were therefore equivalent to a situation in which S = 0. In cases II and III SNRF is independent of S, and thus it is only in Case I that the modified version of the snow model yields a different value of SNRF when compared with the original model.

From model verification procedures, depth of freewater and percentage area of the watershed were found to be related by a factor of S = 0.7 (WHC); where WHC, the water holding capacity of the snowpack, was found to be five percent of the snowpack depth. Model calibration indicated that groundmelt from snowpack takes place at the rate of SNGM = 0.01 inches per day (0.3 mm per day). This quantity of groundmelt was added directly to soil moisture storage.

Channel precipitation

During a storm, part of the precipitation falls close to, or into the stream channel, without being subject to the delaying effects of infiltration and subsurface flow. On the basis of the proportion of total watershed area adjacent to a stream channel, one percent of rainfall was treated as channel precipitation. Surface runoff and channel precipitation are treated as linear reservoirs with a common decay constant, k_s. The linear reservoir is based on the assumption that the rate of discharge from a storage reservoir is proportional to the quantity of water in storage (Figure 13), that is:

$$q = \frac{dS(t)}{dt} = -k_s S(t) \quad . \quad . \quad . \quad . \quad . \quad . \quad (9)$$

in which

q = is the discharge rate from the reservoir
$S(t)$ = is the storage within the basin at any time, t
k_s = is a decay constant for surface runoff and channel precipitation depending upon the basin characteristics (channel precipitation) The value of k_s was established as unity by model verification studies.

Soil moisture

The model allows water entering the root zone to satisfy the retention capacity (M_{cs}) of the soil before interflow and percolation can commence. Only that part of soil moisture which is subject to yearly change is modeled. Thus, soil moisture storage is computed by considering the amount of water removed from the soil profile by interflow, deep percolation, and evapotranspiration and the amount of water added by infiltration and groundmelt from snowpack.

Infiltration

Surface organic conditions, physical characteristics of the soil, and soil moisture conditions influence the capacity rate of infiltration into the root zone at any time, t, (f_r) of water available at the ground surface. Before surface runoff can occur the rate of water supply to the ground surface by rainfall or snowmelt must exceed the capacity infiltration rate. Helvey (1973) reported that no surface runoff was observed before the 1970 fire. When $M_s(t)$, the soil moisture storage at time t is less than saturation capacity (M_{ss}), additional infiltration capacity above the equilibrium rate (f_c) was represented as being proportional to the difference between $M_s(t)$ and M_{ss}. Thus, the capacity infiltration rate (f_r) is computed as follows:

$$f_r = f_c + f_o \frac{(M_{ss} - M_s(t))}{M_{ss}} \quad . \quad . \quad . \quad . \quad . \quad (10)$$

in which f_c is the equilibrium infiltration rate and f_o is the incremental infiltration rate in excess of f_c. The infiltration of water to the soil reduces the soil moisture deficit ($M_{ss} - M_s(t)$), and thus the infiltration rate also is decreased, as indicated by Equation 10 (see Figure 14).

Evapotranspiration

Factors affecting evapotranspiration (ET) include temperature, solar radiation, wind, humidity, and the current soil moisture status. Many techniques of estimating ET are available in the literature. The selection of a particular method usually is restricted by the ability to meet the data requirements of the method.

In the approach adopted for this study, potential evapotranspiration (PET) is computed using the following expression:

$$PET = T_a \frac{CP(m)}{D(m)} \quad . \quad . \quad . \quad . \quad . \quad . \quad . \quad (11)$$

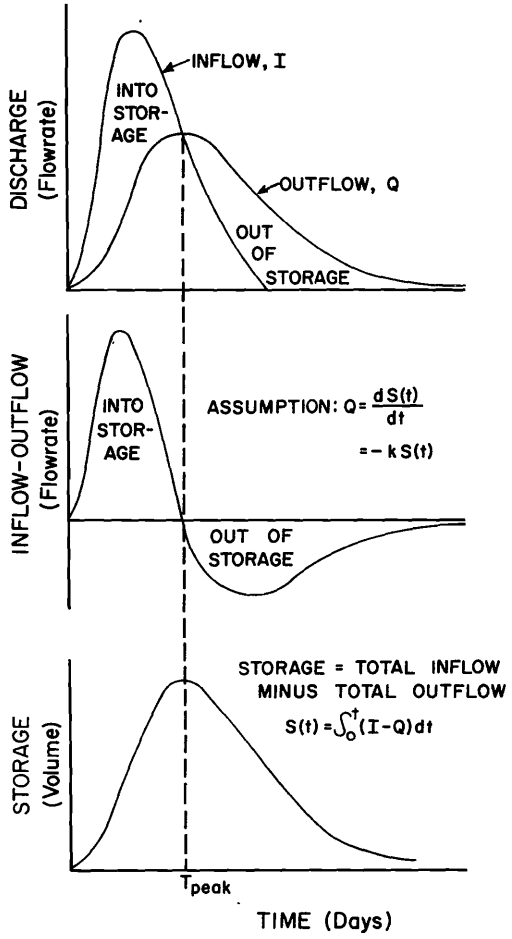

Figure 13. Linear reservoir.

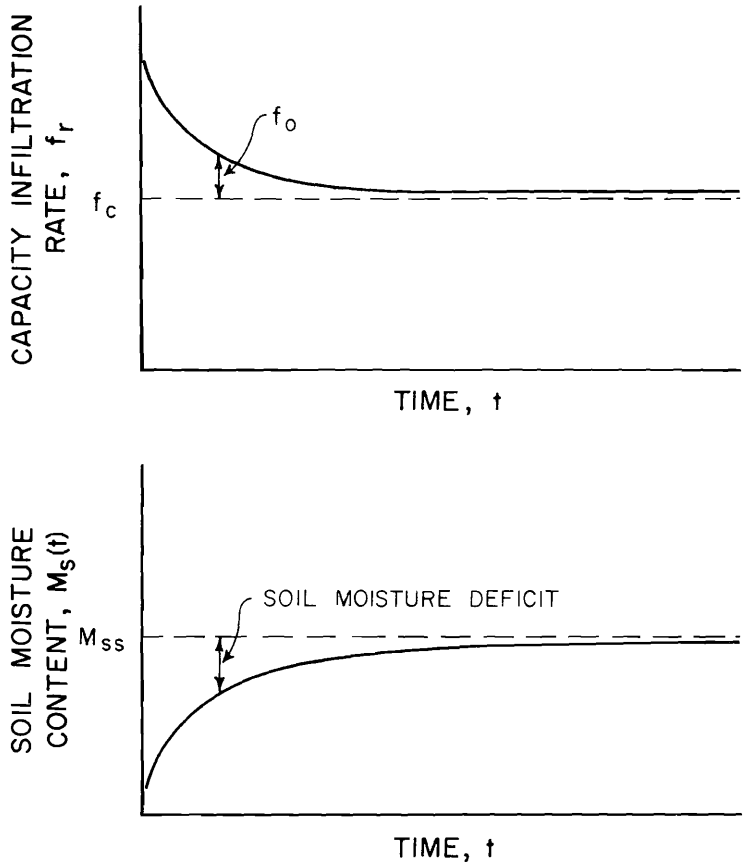

Figure 14. Relationship between reduction in infiltration rate and reduction in soil moisture deficit during a storm of several days duration.

in which T_a is the mean daily air temperature in ^oF; CP(m) is the evapotranspiration per ^oF of mean monthly temperature for the m^{th} month; and D(m) is the number of days in the m^{th} month. PET is satisfied by the following storages in the order in which they are listed: interception storage, snowpack, and soil moisture storage. Thus, if PET exceeds interception storage but is less than the sum of interception and snow storages, then interception storage is depleted, snow storage is reduced by the difference between PET and interception storage, and the ET will equal PET.

In the case where evapotranspiration is taken from soil moisture, ET will equal PET provided soil moisture is above a critical point (M_{es}). This point was found to be two inches (51 mm) through the calibration process. When soil moisture storage ($M_s(t)$) is below M_{es}, that portion of PET which is unsatisfied by interception and snow stoages is reduced by the ratio of $M_s(t)$ to M_{es} according to a technique first proposed by Riley and Chadwick (1967).

The following equations cover each possible case of determining ET from PET based on the status of the interception storage ($S_i(t)$), the snowpack ($M_{sn}(t)$), and the soil moisture storage ($M_s(t)$):

I If $PET \leq S_i(t)$

$$ET = PET \quad (12a)$$
$$S_i(t+1) = S_i(t) - PET \quad (12b)$$
$$M_{sn}(t+1) = M_{sn}(t) \quad (12c)$$
$$M_s(t+1) = M_s(t) \quad (12d)$$

II If $S_i(t) < PET \leq S_i(t) + M_{sn}(t)$

$$ET = PET \quad (13a)$$
$$S_i(t+1) = 0 \quad (13b)$$
$$M_{sn}(t+1) = M_{sn}(t) - (PET - S_i(t)) \quad (13c)$$
$$M_s(t+1) = M_s(t) \quad (13d)$$

III If $S_i(t) + M_{sn}(t) < PET \leq S_i(t) + M_{sn}(t) + (M_s(t) - M_{es})$

$$ET = PET \quad (14a)$$
$$S_i(t+1) = 0 \quad (14b)$$
$$M_{sn}(t+1) = 0 \quad (14c)$$
$$M_s(t+1) = M_s(t) - (PET - S_i(t) - M_{sn}(t)) \quad (14d)$$

IV If $S_i(t) + M_{sn}(t) + (M_s(t) - M_{es}) < PET$ and if

(i) $M_s(t) > M_{es}$

$$ET = S_i(t) + M_{sn}(t) + M_s(t) \quad (15a)$$
$$S_i(t+1) = 0 \quad (15b)$$
$$M_{sn}(t+1) = 0 \quad (15c)$$
$$M_s(t+1) = M_{es} \quad (15d)$$

(ii) $M_s(t) \leq M_{es}$

$$ET = S_i(t) + M_{sn}(t) + \frac{M_s(t)}{M_{es}} (PET - S_i(t) - M_{sn}(t)) \quad (16a)$$
$$S_i(t+1) = 0 \quad (16b)$$
$$M_{sn}(t+1) = 0 \quad (16c)$$
$$M_s(t+1) = M_s(t) - \frac{M_s(t)}{M_{es}} (PET - S_i(t) - M_{sn}(t)) \quad (16d)$$

Interflow

Interflow (N_r) moves laterally within the root zone and reaches a surface channel more quickly than groundwater but less quickly than overland flow. Percolation and interflow, G_s, occur when the soil moisture content (M_s) exceeds the holding capacity of the soil M_{cs}.

Thus:

$$G_s = M_s(t) - M_{cs}, \; M_s(t) > M_{cs} \quad (17a)$$

$$G_s = 0, \; M_s(t) \leq M_{cs} \quad (17b)$$

The combined rate of percolation and interflow, G_d, is estimated by a linear reservoir equation which contains a decay constant, k_g. Thus:

$$G_d = (1 - e^{-k_g}) G_s \quad (18)$$

In the model interflow rate is computed as follows:

$$N_r = G_d - G_r, \; G_s > 0 \quad (19a)$$

$$N_r = 0, \; G_s \leq 0 \quad (19b)$$

in which the rate of percolation (G_r) is given by Equation 23 below.

Baseflow

In the original version of USUWSM baseflow was represented as the outflow from groundwater storage treated as a linear reservoir:

$$BF(t) = -k_b G(t) \quad (20)$$

in which

BF(t) = baseflow at time, t

k_b = linear reservoir decay constant for groundwater storage

$G(t)$ = groundwater storage at time t

However, this model resulted in a poor match between predicted and observed streamflow during the period of low flows occurring between successive snowmelt seasons (Bowles and Riley, 1975). For this period of almost uniform observed flows, predicted streamflow decreased in an approximately exponential fashion. This trend in the computed results was attributed to the low rate at which deep percolation in the model replenishes the groundwater body. The situation can be approximated by a linear reservoir with outflow but no inflow. It can be shown that the outflow, in this case baseflow, decreases in an exponential manner described by:

$$BF(t) = BF(0) \exp(-k_b t) \quad . \quad . \quad . \quad . \quad (21)$$

Substituting Equation 20 into Equation 21 yields

$$BF(t) = -k_b G(0) \exp(-k_b t) \quad . \quad . \quad . \quad (22)$$

On the basis of Equation 22 initial groundwater storage G(0) was made large and k_b was assigned a small value. As a result, the magnitude of predicted baseflow, BF(t), remained fairly steady during the low flow period. However, the snowmelt hydrograph was poorly reproduced due to the excessive dampening of responses from the groundwater reservoir. In addition, the values of initial groundwater storage, G(0), were unrealistically large for the small and steep Entiat watersheds.

The linear reservoir assumption that the rate of baseflow from the groundwater body is proportional to the quantity of water in groundwater storage appeared to be unsuited to the steep Entiat watersheds. While the linear groundwater reservoir functioned well for snowmelt periods, it lacked the capability to reproduce low flows. Therefore, a different approach to the subsurface part of the hydrology simulation model was sought.

The modified view of the streamflow generation process of the steep Entiat watersheds is illustrated in Figures 9 and 15. Baseflow from the saturated groundwater zone was replaced by a quantity termed base percolation. This quantity is sustained by flow from a zone of percolation between the root zone and underlying bedrock. When water infiltrating through the soil surface is insufficient to maintain soil moisture close to its retention capacity, water is withdrawn from the zone of percolation and added to the root zone. Physically this process is explained by capillary conduction under the influence of plant roots. When soil moisture storage exceeds its retention capacity water leaves the root zone by free drainage as interflow and recharge to the underlying zone of percolation. Thus, the effects of capillary movement from the zone of percolation, recharge to the zone of percolation, and, to a lesser extent, interflow are that they tend to maintain the soil moisture storage of the root zone at its retention capacity. These effects are demonstrated by Figure 16, which indicates that soil moisture was supplemented by withdrawals from the zone of percolation during the months of July through October when evapotranspiration was high. Recharge took place during the period of snowmelt and to a lesser extent throughout the entire snow accumulation period.

The rate of interflow is given by Equation 19, and the rate of recharge by percolation, G_r, as follows:

$$G_r = (1 - k''_d) G_d = RH \quad . \quad . \quad . \quad . \quad (23)$$

in which

k''_d = proportion of G_d that becomes interflow

The proportion of G_d that becomes interflow is adjusted to become smaller as the magnitude of the soil moisture surplus $(M_s(t) - M_{cs})$ increases, although the actual amount of interflow continues to increase (Figure 17). This effect is achieved by varying k''_d according to the following equation:

$$k''_d = k'_d \left\{ 1 - \frac{[M_s(t) - M_{cs}]}{M_{ss}} \right\} \quad . \quad . \quad (24)$$

in which

k'_d = value of k''_d approached as $M_s(t)$ approaches M_{cs} from above; dependent on slope and relative magnitudes of vertical and horizontal permability

M_{ss} = saturated soil moisture storage

The rate at which soil moisture is replenished by withdrawal (WD) of water from the zone of percolation is

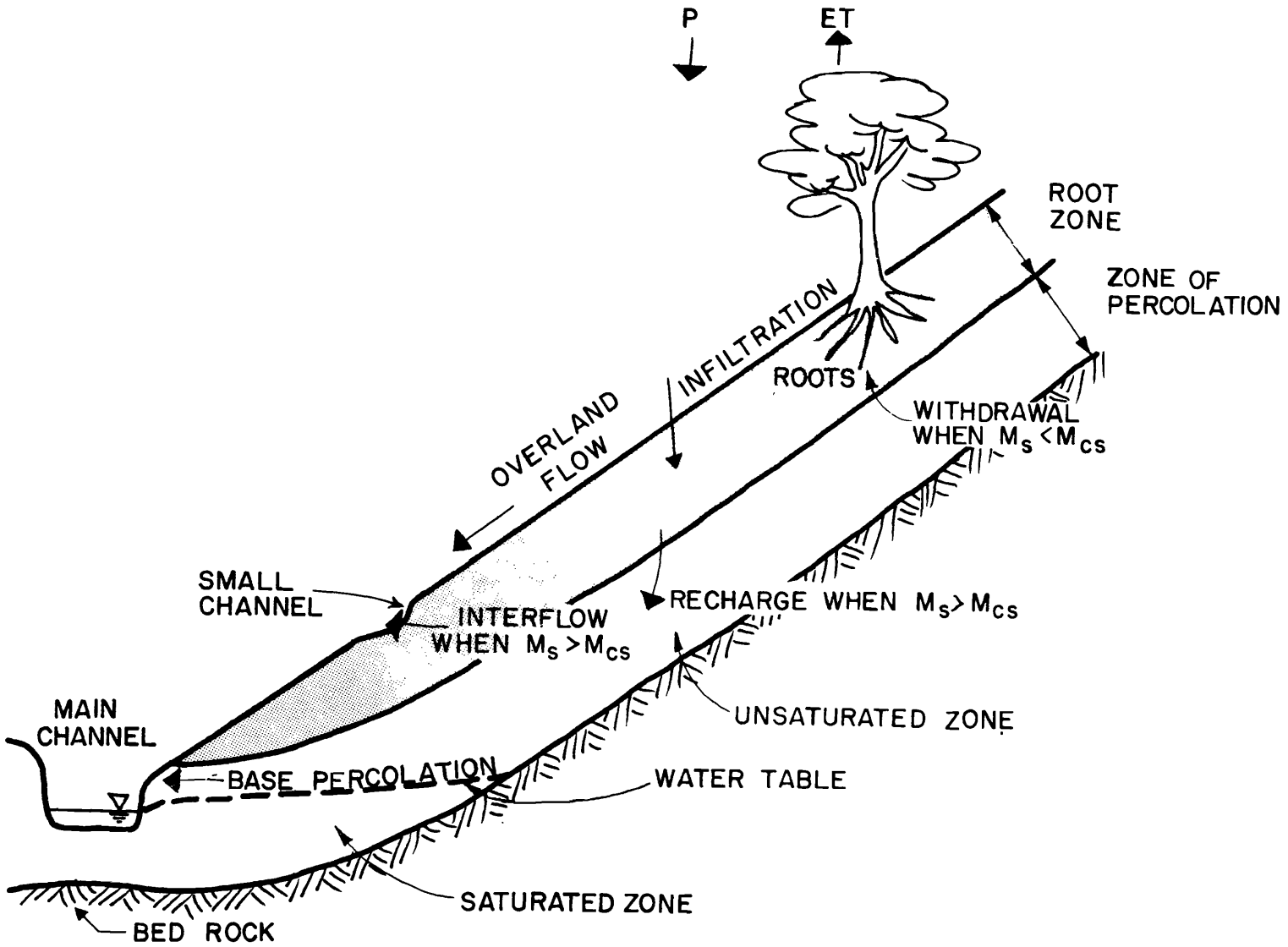

Figure 15. The terrestrial part of the hydrologic cycle in a steep mountain watershed as represented by modified USUWSM

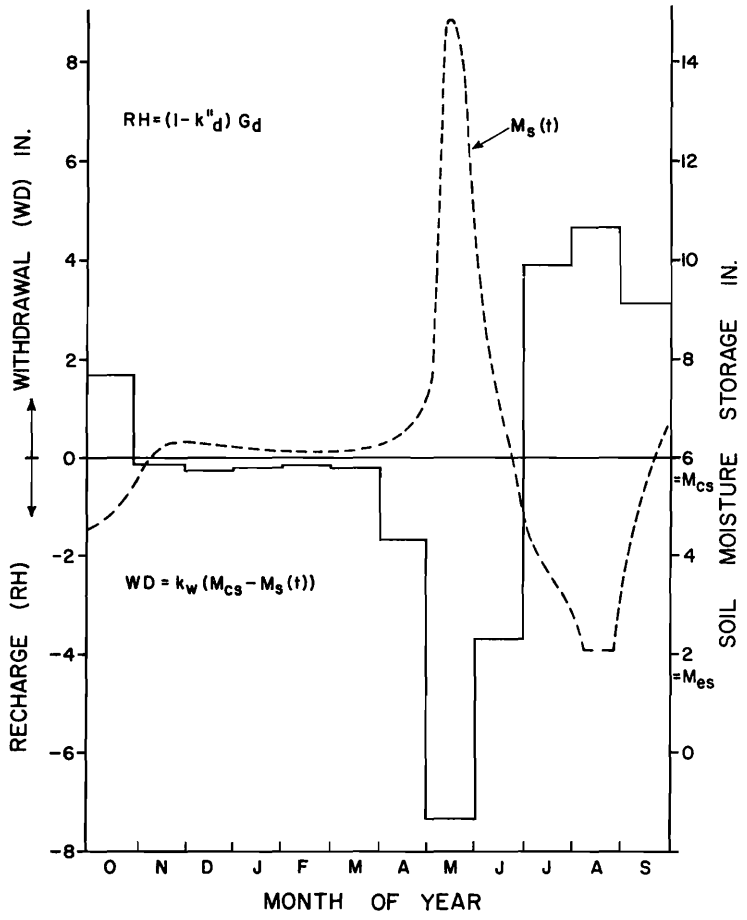

Figure 16. Recharge, withdrawal, and soil moisture storage on McCree Creek, for water year 1964. (1 in. = 25.4 mm).

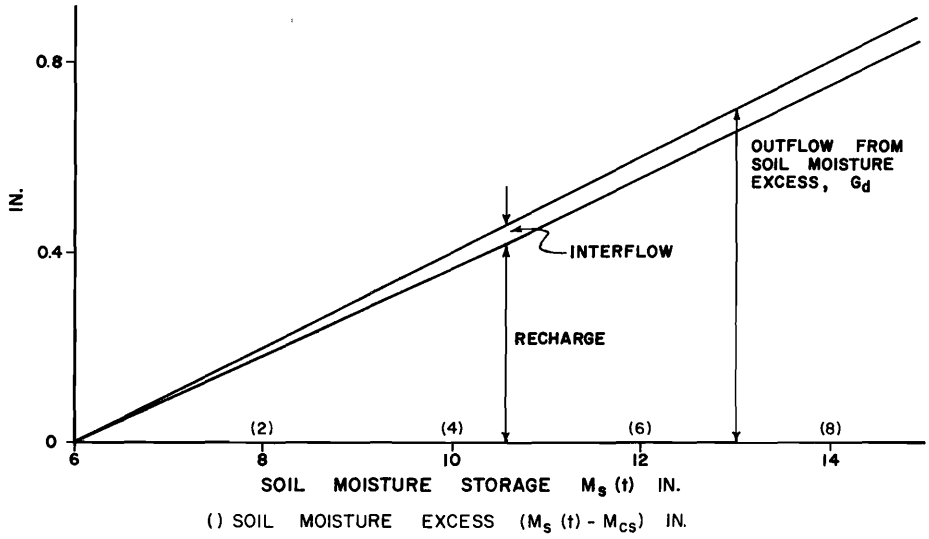

Figure 17. Variation of proportion of outflow from soil moisture excess that becomes interflow and recharge (1 in. = 25.4 mm).

assumed to take place in proportion to the magnitude of the soil moisture deficit:

$$WD = k_w [M_{cs} - M_s(t)], \; M_s(t) < M_{cs} \quad . \quad (25a)$$

$$WD = 0, \; M_s(t) \geq M_{cs} \quad . \quad (25b)$$

in which

k_w = proportion of soil moisture deficit made up by withdrawal

To summarize the conditions for interflow, recharge, and withdrawal, if $M_s(t) < M_{cs}$ then interflow and recharge rates are zero, and the rate of withdrawal from the zone of percolation is given by Equation 25a. If $M_s(t) > M_{cs}$, the withdrawal rate is zero, and the interflow and recharge rates are given by Equation 19a and 23 respectively, with k''_d being given by Equation 24.

Baseflow percolation from the zone of percolation was assumed to be dependent on the history of the total quantity of water stored within that zone. Graupe, Isailovic, and Yevjevich (1975) used a moving average approach to represent the delayed response of a Karst aquifer. A similar approach was adopted in the modified model. Given the present value of a function, F(t), and the (n-1) most recent previous values of that function, the moving average is obtained as follows:

$$\text{Moving average} = \frac{1}{n} \sum_{\tau = t-n+1}^{\tau = t} F(\tau) \quad . (26)$$

Because the magnitude of storage in the zone of percolation was not readily obtainable, the variation of the percolation zone storage was approximated by the variation in soil moisture storage. The justification for the approach was that higher levels of soil moisture storage result in low withdrawals from the zone of percolation, and thus a greater magnitude of storage in that zone. Thus, base percolation was modeled as being proportional to an approximate moving average of soil moisture storage values:

$$SMMA(t) = \frac{(n-1)\, SMMA(t-1) + M_s(t)}{n} \quad . \quad (27)$$

and

$$BP = -k_g \, SMMA(t) \quad . \quad . \quad . \quad . \quad . \quad (28)$$

in which

SMMA(t) = approximate moving average of soil moisture storage at time t

n = number of days on which approximate moving average is based (found to be 90 days by calibration procedure)

k_g = proportion of SMMA(t) that becomes base percolation

The amount of storage in the zone of percolation was not accounted for in the modified model. Only the inflow from soil moisture and outflows to soil moisture and as baseflow were modeled. Therefore, the internal mass balance of the model was lost. However, over an eight year period the simulation results indicated that in the long run inflow to the zone of percolation was approximately equal to outflow. If outflow to soil moisture and as baseflow was consistently greater than inflow from soil moisture this may indicate that water from outside the watershed was entering the zone of percolation.

Initial attempts to model the Entiat watersheds were based on the generally accepted explanation of non-snowmelt streamflow (baseflow) which assumes that extensive, saturated groundwater aquifers feed streams during nonstorm periods. Storm or snowmelt streamflows were assumed to come from overland or subsurface flow through interconnecting channels below the soil surface (interflow).

The difficulty with assuming a linear groundwater reservoir was that, with reasonable values of groundwater storage G(0) for the size of watershed, the predicted streamflow dropped below observed values. This shortcoming was due to the slow rate of replenishment of groundwater storage by deep percolation attributed to extended periods of severe soil moisture deficit. Thus, when soil moisture storage was supplemented by withdrawal from the zone of percolation streamflow predictions were improved.

In an experimental study in deep-soiled areas of the southern Appalachians, Hewlett and Hibbert (1963) "concluded that unsaturated flow in the earth mantle of steep watersheds cannot be ignored in hydrograph analysis, since it may well be a primary mechanism for sustaining baseflow. Groundwater wells at the experimental site failed to show significant saturated aquifers except along streams and drainageways, where accumulated water appears as spring or seepage flow. Because of the steep topography, these areas occur only in the immediate vicinity of the stream, a zone which appears too small to sustain streamflow through the summer period of high evapotranspiration.

In earlier work, Hewlett (1961) proposed an explanation of baseflow which envisages the entire soil mantle as a storage aquifer feeding sus-

tained flow. According to this view, narrow groundwater bodies along stream channels are a conduit through which slowly draining soil moisture passes to enter the stream. This is in contrast to the role of groundwater bodies as the source of baseflow from less steep watersheds.

Hewlett's explanation of the source of baseflow in steep watersheds can be described in terms of the physics of saturated-unsaturated flow in soils. Stephenson and Freeze (1974) have developed a two-dimensional transient mathematical model of the saturated-unsaturated subsurface flow through an instrumented cross-section in the Reynolds Creek Experimental Watershed near Boise, Idaho. Their main conclusion was that "transient saturated-unsaturated subsurface flow can deliver snowmelt infiltration through high-permeability low-porosity formations fast enough to be the sole generating mechanism of runoff from an upstream source area." Data limitations on the Entiat watersheds precluded the use of a complex analysis similar to that of Stephenson and Freeze. In addition, the difficulty in accounting for inhomeogeneities in the hydraulic properties of soils limits the predictive capability of such rigorous techniques applied to real systems (Gardner, 1959).

Streamflow

Channel precipitation, interflow, and surface runoff are summed to obtain the computed streamflow at the stream gage at the bottom of the watershed. No routing of streamflow is necessary since the travel time within each watershed is less than the model time increment of one day.

CHAPTER V

VERIFICATION OF THE MODEL

Model verification includes calibration of the model to a particular area, testing the sufficiency of processes defined in the model, and examination of the predictive performance of the model. Because of the inadequacy of the precipitation input information, the following objectives were established for the model verification procedure:

1. To account for the major portion of the initial variance in the streamflow time series;

2. To achieve the correct timing of the annual snowmelt; and

3. To obtain an approximate water balance over the study period.

At various stages a version of the self-calibrating or optimization algorithm described in Figure 18 was applied (Hill et al., 1971). Under this procedure each unknown model parameter is assigned an initial value, an upper and low bound, and a number of increments to cover the range. The first selected parameter is varied through the specified range while all other parameters remain at their initial values. The values of the objective function (measure of error) for each value of the parameters are printed, and the value of the parameter which produced the minimum objective function is stored. After completion of the runs for the first parameter, the second parameter is taken through the same procedure. After all parameters have been varied, the set of values which produced each local minimum is run and the resultant objective function value is compared with the smallest attained in all previous runs. The vector (values of the parameters) which produced the minimum objective function value is selected as the initial vector for the next phase, and the process is repeated until a parameter vector is found which produces a reasonable correspondence between computed and observed outflows (Hill et al., 1971).

Input to the USUWSM model of this study was daily precipitation and temperature, and output was daily streamflow which may be compared with historical flows. A rough fit first was made using estimated parameter values and initial conditions. Gross adjustments then were made manually before applying the optimization procedure to fix the remaining slack parameter values. A continuous record then was computed to verify the model. When aberrations in output persisted, adjustments were made to the model structure. Table 1 indicates the model parameter values which were established for both pre-fire and post-fire conditions on each of the three study drainage areas.

Two important structural changes were made to the original USUWSM model. As described in the previous chapter, the subsurface component of the model was revised to represent baseflow sustained by unsaturated flow in the earth mantle. A second major alteration to the model was needed because of the importance of snow in the study area. A less sophisticated snowmelt relationship which was used in earlier studies was replaced by the modeling procedure which also was described in the previous chapter. The procedure now used includes groundmelt and freewater in the snowpack which has an important role in the snowmelt process.

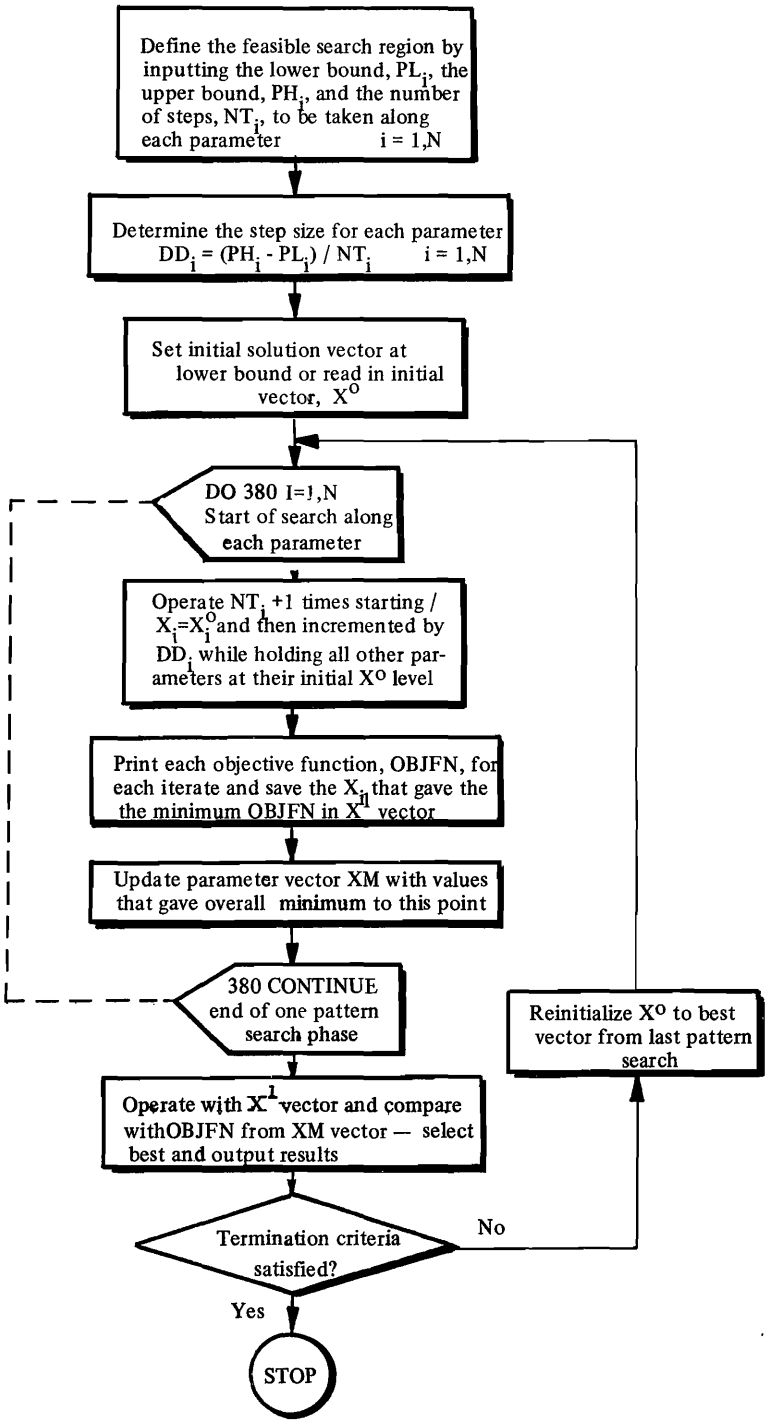

Figure 18. Search algorithm for calibration of hydrologic model (after Hill et al., 1971).

Table 1. Model parameter values for pre-fire and post-fire conditions on the three study watersheds.[1]

Symbol Report	Symbol Program	Description	McCree Pre-fire	McCree Post-fire	Burns Pre-fire	Burns Post-fire[2]	Fox Pre-fire	Fox Post-fire
T_s	TS	Temperature below which all precipitation treated as snow (°F)	30	UNCHANGED THROUGHOUT				
T_r	TR	Temperature above which all precipitation treated as rain (°F)	38					
S_i	SI	Interception storage capacity (ins)	.2	.02	.2	.08	.2	.14
k_s	TSW	Decay constant for surface runoff and channel precipitation; each represented as a linear reservoir	1	1	1	1	1	1
T_m	TMELT	Temperature at which snow melts (°F)	36	32	36	32	36	32
k_m	SMR	Snowmelt coefficient (ins/ °F-day)	.07	.10	.07	.10(.07))	.05	.10
SNGM	SNGM	Daily groundwater melt from snowpack (ins/day)	.01	.01	.01	.01	.01	.01
RI	RAD(M)	Radiation index for m^{th} month M: Oct. 10	.59	UNCHANGED THROUGHOUT				
		Nov. 11	.56					
		Dec. 12	.54					
		Jan. 1	.54					
		Feb. 2	.56					
		Mar. 3	.59					
		Apr. 4	.58					
		May 5	.56					
		June 6	.54					
		July 7	.54					
		Aug. 8	.56					
		Sept. 9	.58					
f_o	FO	Incremental infiltration rate (ins/day)	3	.5	3	.5(1)	3	.5
f_c	FC	Equilibrium infiltration rate (ins/day)	.5	.5	.5	.5	.5	.5

[1] °F = 9/5 °C + 32, 1 in. = 25.4 mm

[2] Post-fire parameter values in parenthesis were developed by considering the pre-fire period under post-fire conditions. Other post-fire parameter values were developed using the post-fire period only.

Table 1. cont.

Symbol Report	Symbol Program	Description		McCree Pre-fire	McCree Post-fire	Burns Pre-fire	Burns Post-fire[2]	Fox Pre-fire	Fox Post-fire
CP(m)	CP(M)	Consumptive use for m^{th} month (ins/ °F)	$\frac{M}{10}$						
		Oct.	10	.030	.020	.030	.020(.014)	.030	.030
		Nov.	11	.010	.010	.010	.010(.009)	.010	.010
		Dec.	12	.000	.000	.000	.000	.000	.000
		Jan.	1	.000	.000	.000	.000	.000	.000
		Feb.	2	.000	.000	.000	.000	.000	.000
		Mar.	3	.000	.000	.000	.000	.000	.000
		Apr.	4	.010	.010	.010	.010(.009)	.010	.010
		May	5	.050	.020	.050	.030(.038)	.050	.040
		June	6	.090	.020	.090	.040(.066)	.090	.070
		July	7	.100	.020	.100	.040(076)	.100	.080
		Aug.	8	.090	.020	.090	.040(.066)	.090	.070
		Sept.	9	.050	.020	.090	.030(.038)	.090	.040
M_{ss}	SS	Saturated soil moisture storage (ins)		15	15	20	20	20	20
M_{cs}	SFC	Soil moisture retention capacity (ins)		6	6	6	6	6	6
M_{es}	WILT	Soil moisture critical point (ins)		2	2	2	2	2	2
k_b	BK	The proportion of AVSM that becomes baseflow		.0010	.0010	.0017	.0017	.0018	.0018
k_i	QK	The proportion of outflow from detention storage which becomes interflow		.14	.14	.15	.15	.16	.16
k_g	TGW	Decay constant for soil moisture excess treated as in linear reservoir		.10	.10	.08	.08	.08	.08

[2]Post-fire parameter values in parenthesis were developed by considering the pre-fire period under post-fire conditions. Other post-fire parameter values were developed using the post-fire period only.

CHAPTER VI

RESULTS

Pre-fire

Table 2 summarizes the results of the model study for the pre-fire period. Table 3 contains definitions for abbreviations used in the sample outputs. As shown by Table 2, if the mean error in prediction of the annual runoff is expressed as a percentage of mean annual runoff, the results for the three drainage areas are as

Table 2. Summary of calibration results for pre-fire period.[1]

	McCree			Burns			Fox		
Year	ER	AE	GWR	ER	AE	GWR	ER	AE	GWR
1963	-.46	1.50	-3.379	-.62	1.70	-3.201	-.71	1.84	-4.106
1964	.02	.84	1.116	-.22	1.10	1.497	-.04	1.52	.641
1965	.35	1.21	-4.199	.05	1.52	-4.025	.32	1.52	-5.059
1966	-.39	.90	5.137	-.72	1.05	5.680	-.83	1.37	4.855
1967	.53	1.46	3.872	.80	2.57	4.222	1.65	3.41	3.439
1968	.35	2.70	-10.715	.38	2.93	-10.791	1.74	3.67	-12.079
1969	.38	2.07	-4.159	1.07	2.51	-3.822	2.65	3.39	4.936
1970	.97	1.11	16.950	1.22	1.61	17.831	1.61	1.89	17.613
Total	1.75	11.79	4.623	1.96	14.99	7.391	6.39	18.61	0.368
Mean	0.22	1.47		0.24	1.87		0.80	2.33	
Mean ER / Mean Runoff	5.15%	34.43%		3.95%	30.76%		11.25%	32.77%	

[1]All units are inches (1 in. = 25.4 mm)

Q_i = observed streamflow on i^{th} day of year

QP_i = predicted streamflow on i^{th} day of year

ER = $\sum_i (Q_i - QP_i)$ i.e. the error in prediction of annual streamflow

AE = $\sum_i |(Q_i - QP_i)|$ i.e. the absolute error in prediction of daily runoff for one year. AE was used as an objective function in the optimization algorithm and may be interpreted as a measure of the distribution of error between computed and observed hydrographs.

GWR = Net withdrawal from the zone of percolation summed over one year. GWR < 0 for net inflow (recharge) to the zone of percolation. GWR > 0 for net outflow (withdrawal) from the zone of percolation. The total GWR is a measure of the water balance over the pre-fire study period.

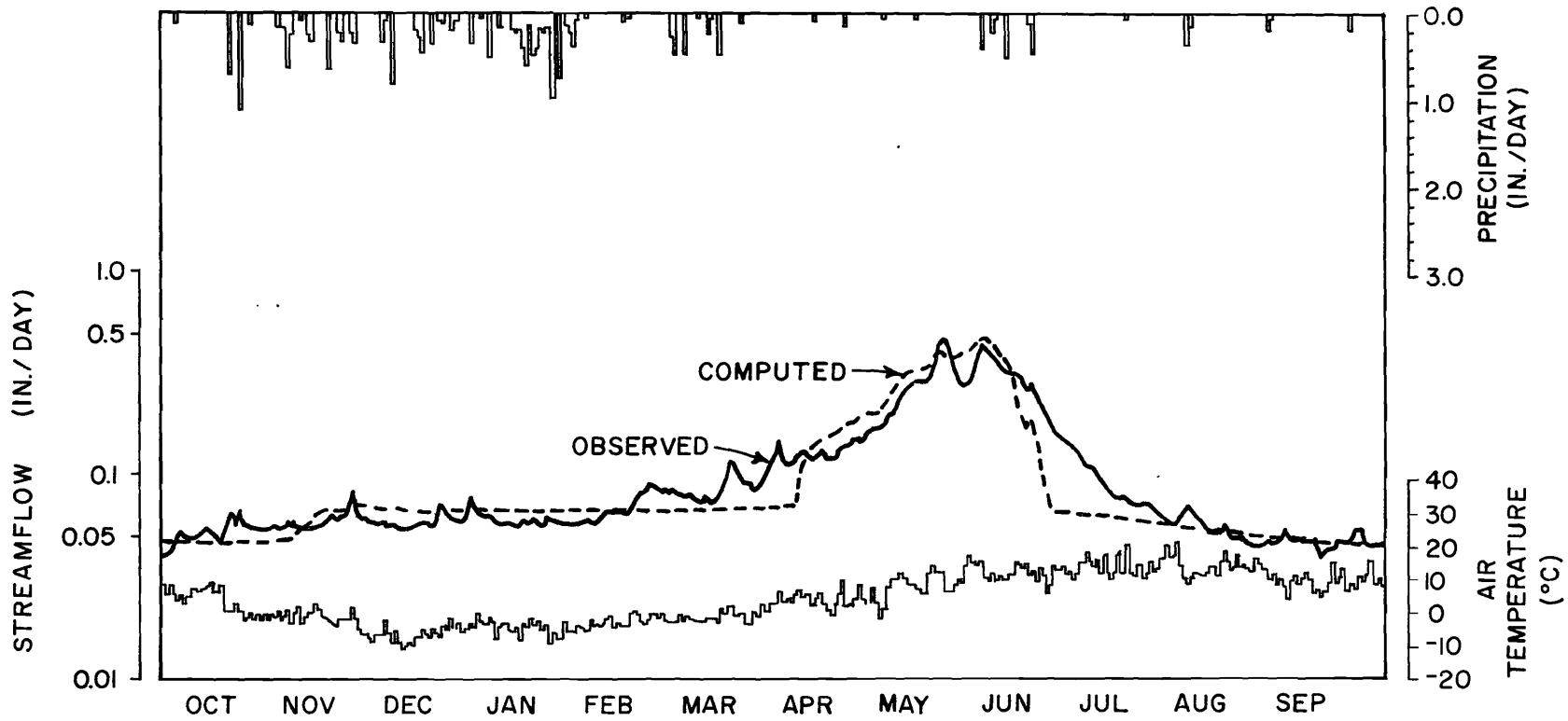

Figure 19. Hydrographs of observed and computed pre-fire streamflow on McCree Creek for the water year 1964 (see Table 4) (1 in. = 25.4 mm, $^{o}C = 5/9\ (^{o}F - 32)$).

Table 4. Pre-fire simulation: tabular output for McCree watershed for water year 1964.[1]

```
MONTHLY WATER BALANCE
  10 PPT 2.61 STM    .16 TEM 36.37 LOSS  2.44 RN    .79 SN  1.81
  11 PPT 4.35 STM    .18 TEM 29.01 LOSS  4.16 RN    .70 SN  3.64
  12 PPT 3.57 STM    .18 TEM 20.42 LOSS  3.38 RN    .00 SN  3.57
   1 PPT 8.11 STM    .19 TEM 23.72 LOSS  7.91 RN    .00 SN  8.11
   2 PPT  .71 STM    .21 TEM 27.09 LOSS   .49 RN    .01 SN   .69
   3 PPT 2.43 STM    .29 TEM 30.43 LOSS  2.13 RN    .11 SN  2.31
   4 PPT  .41 STM    .41 TEM 39.86 LOSS -.00 RN    .35 SN   .05
   5 PPT  .16 STM    .96 TEM 50.70 LOSS -.80 RN    .16 SN   .00
   6 PPT 1.96 STM    .84 TEM 53.91 LOSS 1.11 RN   1.96 SN   .00
   7 PPT  .12 STM    .25 TEM 60.17 LOSS -.13 RN    .12 SN   .00
   8 PPT  .80 STM    .17 TEM 55.52 LOSS  .62 RN    .80 SN   .00
   9 PPT 2.89 STM    .15 TEM 48.93 LOSS  2.73 RN   2.89 SN   .00
YEARLY WATER BALANCE
1964 PPT28.11 STM   4.03 TEM 39.65 LOSS 24.08 RN   7.91 SN 20.20
HYDROLOGIC DATA--MODEL OUTPUT
10
SI    .48  SN  1.74  SM  5.67  GW -1.64  EP  1.15  AV  1.15
SR    .00  TF   .00  BF   .15  PF   .15  ER   .01  AE   .02  VR       .00
11
SI    .41  SN  4.68  SM  6.15  GW   .14  EP   .29  AV   .29
SR    .00  IF   .03  BF   .15  RF   .18  ER  -.00  AE   .02  VR       .00
12
SI    .00  SN  8.24  SM  6.09  GW   .31  EP   .00  AV   .00
SR    .00  IF   .05  BF   .16  RF   .21  ER  -.03  AE   .03  VR       .00
 1-1964
SI    .00  SN 16.04  SM  6.09  GW   .26  EP   .00  AV   .00
SR    .00  IF   .04  BF   .17  RF   .21  ER  -.02  AE   .02  VR       .00
 2
SI    .01  SN 15.44  SM  6.09  GW   .24  EP   .00  AV   .00
SR    .00  IF   .04  BF   .16  PF   .20  ER   .01  AE   .03  VR       .00
 3
SI    .42  SN 18.53  SM  6.09  GW   .26  EP   .00  AV   .00
SR    .00  IF   .04  BF   .18  RF   .22  ER   .06  AE   .06  VR       .00
 4
SI    .32  SN 15.52  SM  7.13  GW  1.78  EP   .39  AV   .39
SR    .00  IF   .26  BF   .17  PF   .44  ER  -.03  AE   .12  VR       .00
 5
SI    .15  SN  1.92  SM 10.09  GW  7.45  EP  2.53  AV  2.53
SR    .00  IF   .93  BF   .19  RF  1.13  ER  -.16  AE   .20  VR       .00
 6
SI   1.01  SN   .00  SM  4.85  GW  3.76  EP  4.85  AV  4.85
SR    .00  IF   .49  BF   .21  PF   .70  ER   .14  AE   .22  VR       .00
 7
SI    .11  SN   .00  SM  2.87  GW -3.91  EP  6.01  AV  6.01
SR    .00  TF   .00  BF   .19  RF   .19  ER   .05  AE   .05  VR       .00
 8
SI    .63  SN   .00  SM  3.26  GW -4.59  EP  4.99  AV  4.99
SR    .00  IF   .00  BF   .17  RF   .17  ER   .00  AE   .01  VR       .00
 9
SI    .49  SN   .00  SM  6.65  GW -3.11  EP  2.44  AV  2.44
SR    .00  IF   .01  BF   .14  RF   .15  ER  -.00  AE   .01  VR       .00
ANNUAL RF  4.01  ER   .02  AE   .84  GWR    1.116  PE 22.68  SI  4.09  AV 22.68
```

[1]See Figure 13 and also Table 3 for definition abbreviations used above. TEM is in ^{o}F ($^{o}F = 9/5\ ^{o}C + 32$). All other units are inches (1 in. = 25.4 mm).

Throughout the study period the model indicated that actual evapotranspiration was equal to potential evapotranspiration. The reason for this was that soil moisture was supplemented by water from the unsaturated zone below the plant roots and hence potential evapotranspiration requirements were always satisfied. Average annual evapotranspiration as predicted by the model was about 23 inches (580 mm). In the simulation of pre-fire years no surface runoff occurred. Some care must be exercised, however, when examining the model predictions for such internal processes as evapotranspiration and surface runoff. The model results can provide only a general picture of the internal processes since no data on these processes were available as a check. In other words, the model of this study is verified only on the basis of streamflow. For example, it is likely that during the late summer when temperatures are high and precipitation is sparce, actual evapotranspiration is less than potential evapotranspiration due to the limiting effect of soil moisture (Helvey, 1973).

Post-fire

One of the advantages of a simulation model is that the effect on streamflow of changes in watershed characteristics may be investigated with considerable ease and economy. These effects are studied by making changes to model parameters to represent the changes in watershed characteristics. Model output using the new parameter values shows the predicted effects on the streamflow of the watershed alterations. Examples of these watershed changes are the introduction of a reservoir, channel improvements, urbanization, diversions, and vegetation management.

For this study, Table 1 shows the changes made to model parameters for the post-fire simulation. In the table post-fire parameter values shown in parenthesis were obtained for the pre-fire period of data under assumed post-fire conditions; other post-fire parameter values were developed using the post-fire period of data. These changes were to parameters related to watershed characteristics that were affected by the fire.

In a similar study (Fleming, 1971) of two extensively burned watersheds in California, evapotranspiration and interception storage related parameters were reduced to account for streamflow changes. In establishing values of monthly evapotranspiration per °F (CP) and interception storage (S_i) Fleming assumed the complete elimination of vegetation from the two watersheds. In the case of the Entiat study, it was estimated from field observations that vegetation cover on the McCree, Burns, and Fox Creek watersheds were 100 percent, 70 percent, and 30 percent destroyed, respectively. Post-fire values for CP and S_i then were calculated by interpolation between the estimated values for pre-fire conditions and those for complete vegetation removal, according to the percentage of vegetation destroyed. Berndt (1971), commenting on the effects of the Entiat forest fire, stated "that a reduction of evaporation from the soil by a deep ash mulch could have influenced streamflow after the fire."

Other parameter changes required for post-fire conditions were to the snowmelt coefficient and the incremental infiltration rate. In the absence of a forest canopy an increased quantity of solar energy will reach the snowpack surface. Previous studies (Riley and Chadwick, 1967; U.S. Army Corps of Engineers, 1956; and U.S. Army Corps of Engineers, 1960) indicate a relationship between the vegetation canopy density (C_v) and the snowmelt coefficient (k_m), such that:

$$k_m = C \exp(-4C_v) \quad . \quad . \quad . \quad . \quad . \quad (29)$$

where C is a proportionality constant. Hence, in this study to represent post-fire conditions, the snowmelt coefficient (k_m) was increased, and the temperature at which snowmelt occurs (T_m) was reduced.

Klock (1971) has observed that "since the fire considerable carbonized plant material (ash) covers the soil surface, particularly in the stream zones." The incremental infiltration rate, f_o, was reduced to represent the sealing effect of ash on the soil surface (Figure 14). Settergren (1967) indicates that a reduction in infiltration rate is a usual result of forest fires in areas of coarse soils. The fine ash resulting from the fire is washed into the soil pores, and then becomes compacted by raindrop impact. Thus, because the total infiltration value is reduced, the responsiveness of the hydrologic system is increased.

Figure 20 contains hydrographs of observed pre-fire streamflow and computed post-fire streamflow on Burns Creek for the 1964 water year (see also Tables 5 and 6). The difference between the two hydrographs represents the predicted change in streamflow as a result of the fire. Because differences usually are more reliable than absolute values, the computed post-fire streamflow hydrograph was obtained by adding the algebraic difference between the simulated post-fire and simulated pre-fire runoff hydrographs to the observed pre-fire runoff hydrographs.

Due to the short period of data available for calibration of post-fire conditions, the results of the post-fire simulation should be viewed qualitatively rather than quantitively. The model results indicate a slight increase in the responsiveness of streamflow

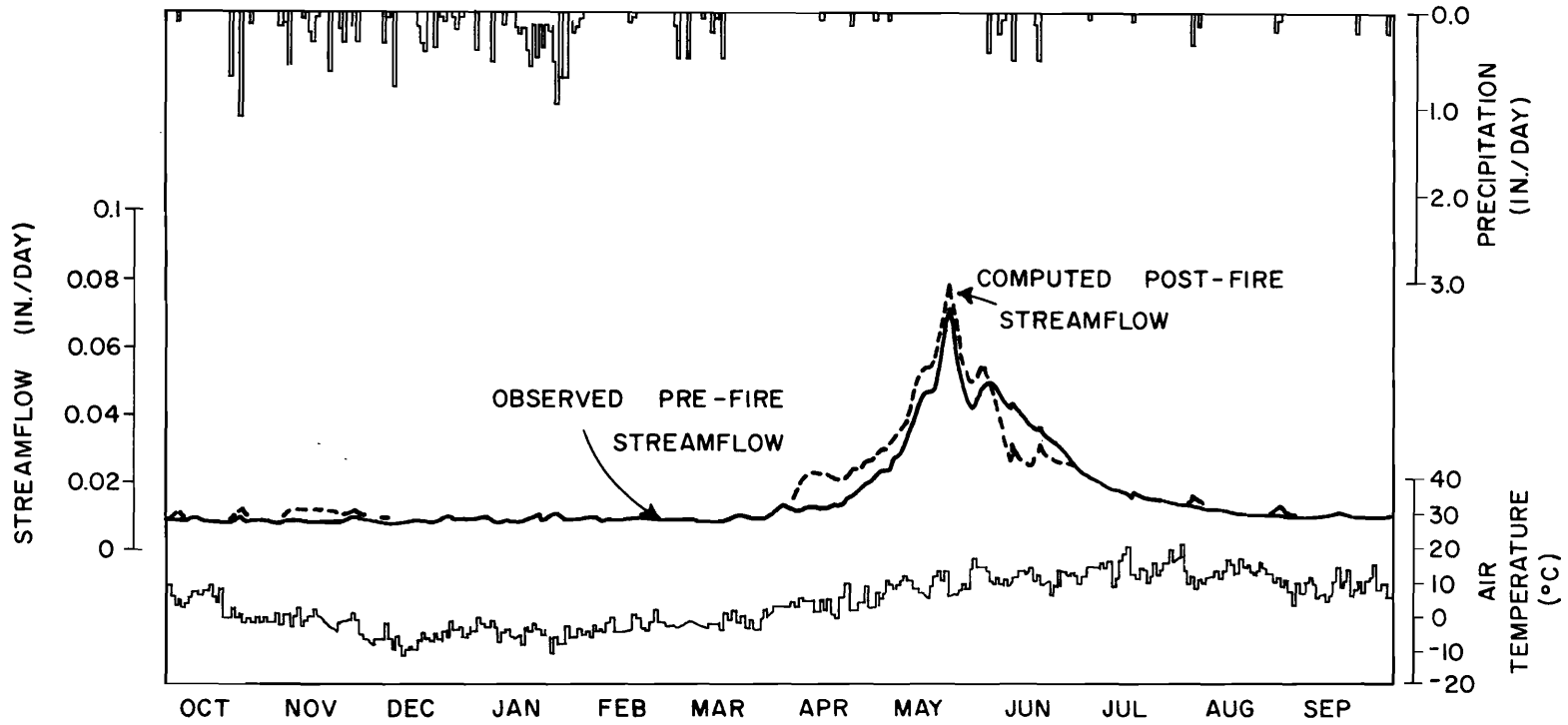

Figure 20. Hydrographs of observed pre-fire streamflow and computed post-fire streamflow on Burns Creek for water year 1964 (see Tables 5 and 6) (1 in. = 25.4 mm, $^{o}C = 5/9 (^{o}F - 32)$).

Table 5. Pre-fire simulation: tabular output for Burns watershed for water year 1964.[1]

```
MONTHLY WATER BALANCE
  10 PPT 2.75 STM   .26 TEM 37.87 LOSS  2.48 RN   .68 SN  2.06
  11 PPT 4.62 STM   .26 TEM 28.41 LOSS  4.35 RN   .59 SN  4.02
  12 PPT 3.72 STM   .26 TEM 19.92 LOSS  3.45 RN   .00 SN  3.72
   1 PPT 8.48 STM   .27 TEM 23.22 LOSS  8.20 RN   .00 SN  8.48
   2 PPT   .73 STM   .25 TEM 26.59 LOSS   .47 RN   .01 SN   .72
   3 PPT 2.58 STM   .28 TEM 30.03 LOSS  2.29 RN   .10 SN  2.47
   4 PPT   .45 STM   .44 TEM 39.46 LOSS   .01 RN   .37 SN   .07
   5 PPT   .16 STM  1.36 TEM 50.30 LOSS -1.20 RN   .16 SN   .00
   6 PPT 2.05 STM  1.06 TEM 53.61 LOSS   .98 RN  2.05 SN   .00
   7 PPT   .12 STM   .49 TEM 59.87 LOSS  -.37 RN   .12 SN   .00
   8 PPT   .84 STM   .33 TEM 55.22 LOSS   .50 RN   .84 SN   .00
   9 PPT 3.02 STM   .27 TEM 48.43 LOSS  2.74 RN  3.02 SN   .00
YEARLY WATER BALANCE
1964 PPT29.91 STM  5.60 TEM 39.41 LOSS 23.91 RN  7.96 SN 21.55
HYDROLOGIC DATA--MODEL OUTPUT
10
SI   .25  SN  1.82  SM  5.91  GW -1.85  EP  .98  AV  .98
SR   .00  IF   .00  BF   .28  RF   .29  ER -.03  AE  .03  VR       .00
11
SI   .26  SN  3.45  SM  6.18  GW   .35  EP  .25  AV  .25
SR   .02  IF   .06  BF   .28  RF   .35  ER -.09  AE  .09  VR       .00
12
SI   .33  SN  8.36  SM  6.12  GW   .31  EP  .00  AV  .00
SR   .10  IF   .05  BF   .34  RF   .35  ER -.09  AE  .09  VR       .00
 1-1964
SI   .22  SN 17.43  SM  6.12  GW   .26  EP  .00  AV  .00
SR   .00  IF   .04  BF   .30  RF   .35  ER -.07  AE  .07  VR       .00
 2
SI   .01  SN 17.46  SM  6.12  GW   .24  EP  .00  AV  .00
SR   .00  IF   .04  BF   .29  RF   .33  ER -.07  AE  .07  VR       .00
 3
SI   .26  SN 19.79  SM  6.12  GW   .26  EP  .00  AV  .00
SR   .00  IF   .04  BF   .31  RF   .36  ER -.07  AE  .07  VR       .00
 4
SI   .25  SN 14.65  SM  7.94  GW  2.90  EP  .35  AV  .35
SR   .00  IF   .46  BF   .31  RF   .78  ER -.33  AE  .34  VR       .00
 5
SI   .15  SN   .00  SM 10.91  GW  8.80  EP 1.91  AV 1.91
SR   .00  IF  1.16  BF   .36  RF  1.52  ER -.15  AE  .25  VR       .00
 6
SI   .48  SN   .00  SM  5.47  GW  3.41  EP 3.53  AV 3.53
SR   .00  IF   .50  BF   .38  RF   .91  ER  .15  AE  .23  VR       .00
 7
SI   .09  SN   .00  SM  3.71  GW -2.67  EP 4.55  AV 4.55
SR   .00  IF   .00  BF   .36  RF   .36  ER  .12  AE  .12  VR       .00
 8
SI   .33  SN   .00  SM  4.10  GW -3.20  EP 3.64  AV 3.64
SR   .00  IF   .00  BF   .32  RF   .33  ER  .00  AE  .01  VR       .00
 9
SI   .23  SN   .00  SM  6.20  GW -2.28  EP 1.84  AV 1.84
SR   .77  IF   .00  BF   .28  RF  1.08  ER -.00  AE  .80  VR       .02
ANNUAL PP  7.36  ER -1.46  AE  2.22  GWR   -3.610  PE 17.00  SI  2.36  AV 17.00
```

Table 6. Post-fire simulation: tabular output for Burns watershed for water year 1964.[1]

```
MONTHLY WATER BALANCE
  10 PPT 2.75 STM   .26 TEM 37.87 LOSS  2.48 RN   .68 SN  2.06
  11 PPT 4.62 STM   .26 TEM 28.41 LOSS  4.35 RN   .59 SN  4.02
  12 PPT 3.72 STM   .26 TEM 19.92 LOSS  3.45 RN   .00 SN  3.72
   1 PPT 8.48 STM   .27 TEM 23.22 LOSS  8.20 RN   .00 SN  8.48
   2 PPT   .73 STM   .25 TEM 26.59 LOSS   .47 RN   .01 SN   .72
   3 PPT 2.58 STM   .28 TEM 30.03 LOSS  2.29 RN   .10 SN  2.47
   4 PPT   .45 STM   .44 TEM 39.46 LOSS   .01 RN   .37 SN   .07
   5 PPT   .16 STM  1.36 TEM 50.30 LOSS -1.20 RN   .16 SN   .00
   6 PPT 2.05 STM  1.06 TEM 53.61 LOSS   .98 RN  2.05 SN   .00
   7 PPT   .12 STM   .49 TEM 59.87 LOSS  -.37 RN   .12 SN   .00
   8 PPT   .84 STM   .33 TEM 55.22 LOSS   .50 RN   .84 SN   .00
   9 PPT 3.02 STM   .27 TEM 48.43 LOSS  2.74 RN  3.02 SN   .00
YEARLY WATER BALANCE
1964 PPT29.91 STM  5.60 TEM 39.41 LOSS 23.91 RN  7.96 SN 21.55
HYDROLOGIC DATA--MODEL OUTPUT
10
SI   .25  SN  1.82  SM  5.91  GW -1.85  EP  .98  AV  .98
SR   .00  IF   .00  BF   .28  RF   .29  ER -.03  AE  .03  VR       .00
11
SI   .26  SN  3.45  SM  6.18  GW   .35  EP  .25  AV  .25
SR   .02  IF   .06  BF   .28  RF   .35  ER -.09  AE  .09  VR       .00
12
SI   .33  SN  8.36  SM  6.12  GW   .31  EP  .00  AV  .00
SR   .10  IF   .05  BF   .34  RF   .35  ER -.09  AE  .09  VR       .00
 1-1964
SI   .22  SN 17.43  SM  6.12  GW   .26  EP  .00  AV  .00
SR   .00  IF   .04  BF   .30  RF   .35  ER -.07  AE  .07  VR       .00
 2
SI   .01  SN 17.46  SM  6.12  GW   .24  EP  .00  AV  .00
SR   .00  IF   .04  BF   .29  RF   .33  ER -.07  AE  .07  VR       .00
 3
SI   .26  SN 19.79  SM  6.12  GW   .26  EP  .00  AV  .00
SR   .00  IF   .04  BF   .31  RF   .36  ER -.07  AE  .07  VR       .00
 4
SI   .25  SN 14.65  SM  7.94  GW  2.90  EP  .35  AV  .35
SR   .00  IF   .46  BF   .31  RF   .78  ER -.33  AE  .34  VR       .00
 5
SI   .15  SN   .00  SM 10.91  GW  8.80  EP 1.91  AV 1.91
SR   .00  IF  1.16  BF   .36  RF  1.52  ER -.15  AE  .25  VR       .00
 6
SI   .48  SN   .00  SM  5.47  GW  3.41  EP 3.53  AV 3.53
SR   .00  IF   .50  BF   .38  RF   .91  ER  .15  AE  .23  VR       .00
 7
SI   .09  SN   .00  SM  3.71  GW -2.67  EP 4.55  AV 4.55
SR   .00  IF   .00  BF   .36  RF   .36  ER  .12  AE  .12  VR       .00
 8
SI   .33  SN   .00  SM  4.10  GW -3.20  EP 3.64  AV 3.64
SR   .00  IF   .00  BF   .32  RF   .33  ER  .00  AE  .01  VR       .00
 9
SI   .23  SN   .00  SM  6.20  GW -2.28  EP 1.84  AV 1.84
SR   .77  IF   .00  BF   .28  RF  1.08  ER -.00  AE  .80  VR       .02
ANNUAL PP  7.36  ER -1.46  AE  2.22  GWR   -3.610  PE 17.00  SI  2.36  AV 17.00
```

[1]See Figure 14 and also Table 3 for definition of abbreviations used above. TEM is in ^{o}F ($^{o}F = 9/5\ ^{o}C + 32$). All other units are inches (1 in. = 25.4 mm).

to precipitation, with both flood peaks and flood volumes being increased in periods of above-freezing temperatures. Also, post-fire snowmelt occurs earlier in the season and results in higher streamflow rates than was the case for pre-fire conditions. Fleming (1971), Beatty (1967), and Hansen (1968) have also observed that the removal of vegetation has increased the water yield of watersheds.

CHAPTER VII

DISCUSSION, RECOMMENDATIONS, AND CONCLUSIONS

Discussion

There are two limitations to be considered when examining the results of a simulation study:

1. The representativeness of the data; and

2. The adequacy of the model structure and calibration.

Data preparation is described at the beginning of this report. Spatial distribution of precipitation was based on stations located approximately 30 miles (48 km) from the study area. Normally, a more reliable distribution would be expected from the gages on the study area. However, the available records from these were too short to derive a meaningful method for distributing the measured precipitation. This situation represents a severe limitation to the simulation study. Streamflow was measured at a single point on each watershed and was therefore considered to be more accurate than estimated precipitation.

Despite the limitation of inadequate data to estimate the spatial distribution of precipitation, reasonable agreement was achieved between observed and simulated streamflow, both in terms of the overall timing and quantity. To achieve these results it was necessary to make some structural changes to the Utah State University Watershed Simulation Model (USUWSM). In particular, changes were made in the representations of the subsurface hydrology and snowmelt processes. In addition, changes, were made to some of the storages functions as they are affected by evapotranspiration.

With the significant difference in elevation on each of the three study watersheds, it is expected that the representation of the hydrologic system would be improved through the use of a distributed parameter, rather than a lumped parameter, model. In this case, however, the data inadequacy precluded the use of spatially high resolution models.

Post-fire results indicated a slight increase in the responsiveness of streamflow to precipitation with both flood peaks and flood values being increased in periods of above freezing temperatures. This change can be attributed to two factors, namely (1) reduced evapotranspiration resulting from the destruction of vegetation, and the accumulation of ash on the soil surface, and (2) reduced infiltration rates and consequent increases in overland flow on the post-fire watersheds. Also, post-fire snowmelt occurs earlier and is associated with higher streamflow rates than was the case for pre-fire conditions. This change is due mainly to the loss of shading from vegetation which was removed by the fire. Thus, snowmelt occurs more rapidly than was the case under pre-fire conditions. Because they are based on a very short period of post-fire record, a cautionary note must be applied to the above conclusions on the effects of the fire on the runoff characteristics.

Recommendations

As a result of the simulation experience on the Entiat Experimental Watershed, the following recommendations are made:

1. A fairly dense precipitation data network should be established on the experimental watersheds. A period of record of four or five years might be expected to yield a realistic spatial distribution of precipitation in terms of model input.

2. In the light of Hewlett and Hibbert's findings, some further changes to the modified model are proposed. The linear groundwater reservoir removed in the earlier model changes will be replaced. Base percolation will enter the saturated groundwater body close to the stream and outflow from this linear groundwater reservoir will be baseflow. Instead of the indirect method of calculating base percolation from the approximate moving average of soil moisture, the approximate moving average of percolation zone storage itself will be used in Equations 27 and 28. This more flexible model will facilitate investigation of the relative importance of unsaturated flow to the generation of low flows from a particular watershed and will restore the model's internal mass balance. It is considered that it also will improve prediction of the snowmelt hydrograph

recession which was over-dampened in the new model. Figure 21 contains a comparison of the initial, new (current), and proposed models.

3. A hydrogeological investigation is recommended into the subsurface water regime of the study area. This investigation should be aimed at achieving a better understanding of the causative factors associated with the unresponsiveness of streamflow to precipitation. Special attention should be given to identifying saturated and unsaturated subsurface zones and to the measurement of soil moisture tension variation with time and elevation. These data either would help to confirm that baseflow is sustained by unsaturated flows in the earth or would provide an alternative explanation.

4. As post-fire data continues to accumulate, it will be possible to further check and improve the simulation of post-fire conditions, and also to study the dynamic effects of vegetation regrowth on streamflow characteristics.

Conclusions

The study has demonstrated the potential utility of the simulation approach for investigating the physical processes behind changes in runoff characteristics resulting from the effects of fire and other possible management changes on a forest watershed. In this regard, Figure 22 demonstrates the development process of a hydrologic model. It is a continuous process which includes feedback loops. Several of the loops shown in Figure 22 were utilized in this study. In particular, the improvement of system definition was necessary in the subsurface and snow models. The modeling effort has shown data deficiencies for establishing a precipitation distribution relationship and for calibrating the watershed under post-fire conditions. Also, this study has shown a need for a better understanding of the subsurface flow regime of the experimental watershed. As these data and knowledge deficiencies at the study area are satisfied, and as fire-hydrology relationships become better understood, the predictive capability of the USUWSM as applied to this area will be enhanced. Further simulation studies should place greater emphasis on the role of vegetation, and in particular, the post-fire vegetation succession and its effects on hydrologic characteristics.

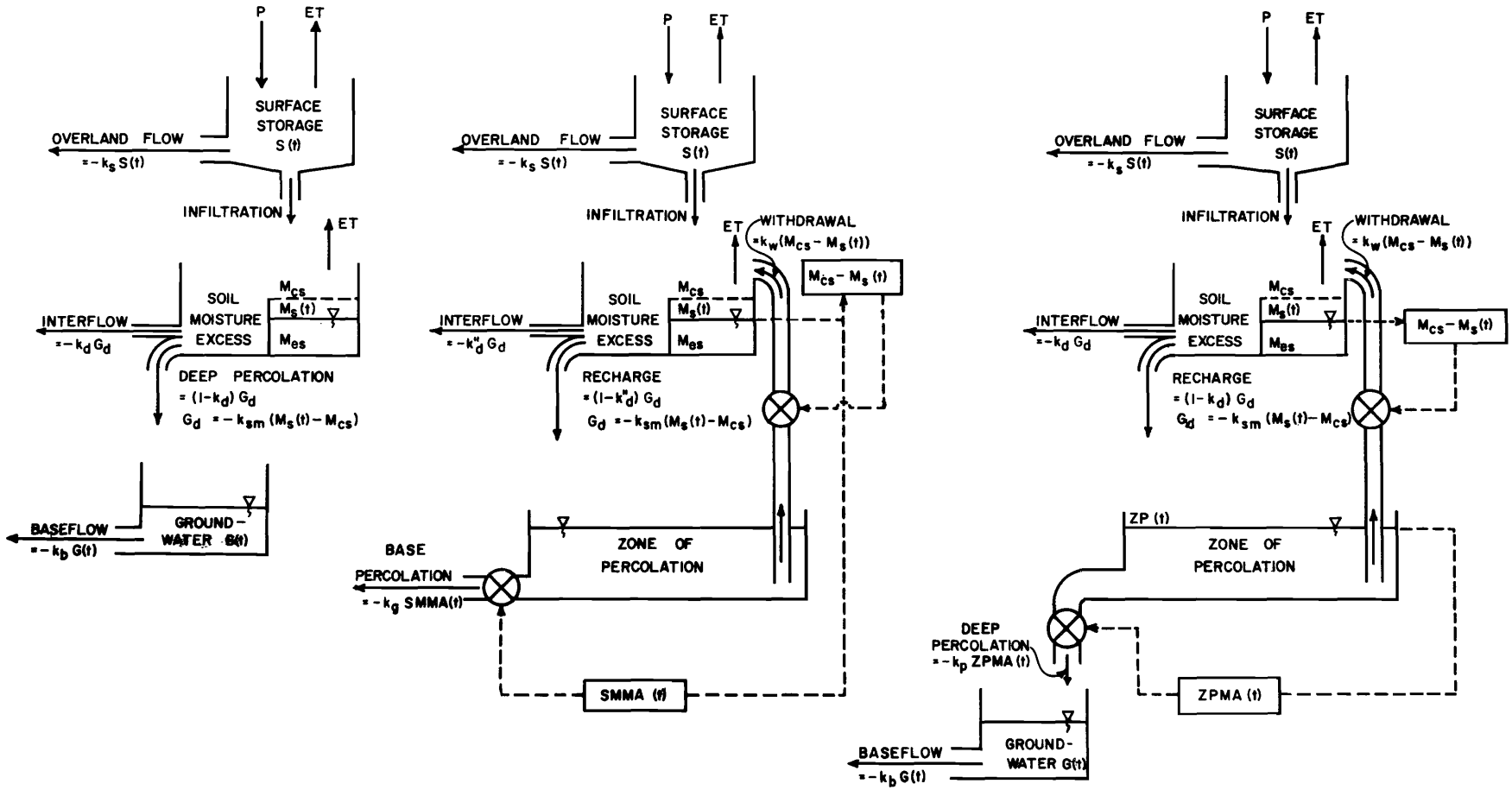

a) Initial version

b) New (current) version

c) Proposed version

Figure 21. Comparison of the flow diagrams for the initial, new, and proposed versions of the watershed hydrologic model.

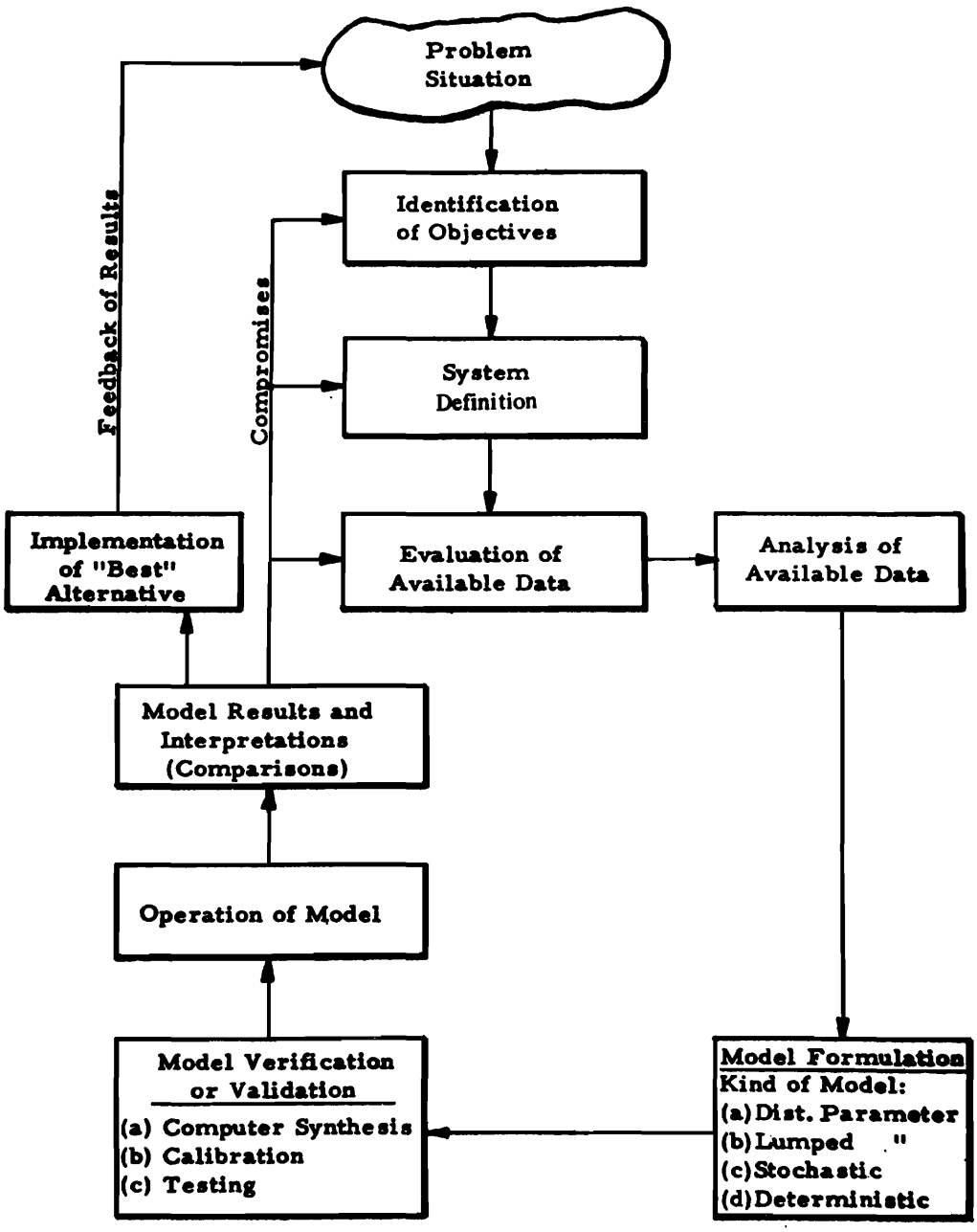

Figure 22. Development process of a hydrologic model (after Riley, 1970).

SELECTED REFERENCES

Amorocho, J., and B. Espildora. 1966. Mathematical simulation of the snow melting processes. Water Sci. Eng. Pap. 3001, Univ. California, Davis.

Anderson, E.A., and N H. Crawford. 1964. The synthesis of continuous snowmelt runoff hydrographs on a digital computer. Tech. Rep. 36, Dept. Civ. Eng., Stanford Univ., Standford, Calif.

Beatty, B. 1967. Increased water yields and improved timing of streamflow through manipulation of forestry vegetation and snowpack management. International Conference on Water Peace, Paper 646, Washington, D.C. 8 p.

Berndt, H.W. 1971. Early effects of forest fire on streamflow characteristics. USDA Forest Service Research Note PNW-148. Pacific Northwest Forest and Range Experiment Station, Portland, Oregon. 9 p.

Bowles, D.S., and J.P. Riley. 1975. An approach to low flow modeling in small steep watersheds. Presented at American Society of Civil Engineers Annual Convention, Denver, Colorado, November, and accepted by Journal of the Hydraulics Division, ASCE.

Carter, R.W. and R.G. Godfrey. 1960. Storage and flood routing , manual of hydrology: Part 3, Flood-flow techniques. Geological Survey Water-supply paper 1543-B. p. 83.

Chambers, M.D. 1973. Computer simulation of the hydrologic system of a mountain watershed. Unpublished M.S. Thesis Utah State University Library, Logan, Utah.

Eggleston, K.O., E.K. Israelsen and J.P. Riley. 1971. Hybrid computer simulation of the accumulation and melt processes in a snowpack. PRWG 65-1, Utah Water Res. Lab., Utah State University, Logan, Utah. 77 p.

Fleming, G. 1971. Simulation of water yield from devegetated basins. Proc. A.S.C.E., Vol. 97, No. IR2, June.

Fryxell, R. 1965. Mazana and glacier peak volcanic ash layers: Relative ages. Science 147:1288-1290.

Graupe, D., D. Isailovic, and V. Yevjevich. 1975. Prediction model for runoff from karstified catchments. Paper presented at Bilateral United States-Yugoslovian Seminar in Karst Hydrology and Water Resources Dubrovnik, Yugoslavia, June 1975. 17 p.

Hansen, W.H. 1968. Santa Ynez barometer watershed. Presented at the 12th Annual Arizona Watershed Symposium, Phoenix, Arizona. September 18.

Helvey, J.D. 1973. Watershed behavior after forest fire in Washington. Proceedings of the Irrigation and Drainage Division Specialty Conference, Fort Collins, Colorado. April 22-24. pp 403-422.

Hewlett, J.D. 1961. Soil moisture as a source of baseflow from steep mountain watersheds. Southeastern Forest Experiment Station, Forest Service, U.S.D.A., Asheville, North Carolina Station paper no. 132. 11 p.

Hewlett, J.D., and A.R. Hibbert. 1963. Moisture and energy conditions within a sloping soil mass during drainage. Journ. Geophys. Res. 68:1081 1087.

Hill, R.W., E.K. Israelsen, A.L. Huber, and J.P. Riley. 1971. A hydrologic model of the Bear River Basin. PRWG72-1, Utah Water Res. Lab., Utah State University, Logan, Utah.

Iritani, D.Y., and L.C. Meyer. 1967. Soil management report, Entiat area. USDA Forest Service, Pacific Northwest Region Report. 164 p.

Klock, G.O. 1971. Streamflow nitrogen loss following forest erosion control fertilization. Publ. PNW-169. USDA Forest Service Research Note, Pacific Northwest Forest and Range Experiment Station.

Lee, R. 1963. Evaluation of solar beam radiation as a climatic parameter of mountain watersheds. Hydrology Papers, No. 2, Colorado State University, Fort Collins, Colorado. 50 p.

Page, B.M. 1939. Geology of a part of the Chiwaukum quadangle. Unpublished Ph.D. thesis on file at Stanford University, Palo Alto, California.

Pysklywec, D.W., K.S. Davar, and D.I. Bray. 1968. Snowmelt index plot. Water Resour. Res. 4:5.

Riley, J.P., D.G. Chadwick, and J.M. Bagley. 1966. Application of electronic analog computer to solution of hydrologic and river-basin-planning problems: Utah simulation model II. PRWG32-1, UWRL, Logan, Utah.

Riley, J.P., and D.G. Chadwick. 1967. Application of an electronic analog computer to the problems of river basin hydrology. PRWG46-1, Utah Water Research Laboratory, Logan, Utah, December. 199 p.

Riley, J.P. 1970. Computer simulation of water resource systems. In Systems Analysis of Hydrologic Problems, Proceedings of the Second International Seminar for Hydrology Professors, held at Utah State University. August 2-14. pp. 249-274.

Riley, J.P., V.J. Rogers, and G.B. Shih. 1974. Hydrologic model studies of the Mt. Olympus Cove Area of Salt Lake County. PRWG134-1. Utah Water Research Laboratory, College of Engineering, Utah State University, Logan, Utah.

Settergren, C.D. 1967. Effects of fire on wildland hydrology. PhD. Thesis, Colorado State University. 218 p.

Shih, D.D. 1971. A simulation model for predicting the effects of weather modification on runoff characteristics. PhD. dissertation, Utah State University, Logan, Utah.

Shih, C.C., R.H. Hawkins, and M.D. Chambers. 1972. Computer modeling of a coniferous forest watershed. "Age of changing priorities for land and water," Irrigation and Drainage Division Specialty Conference, Spokane, Washington.

Twedt, T. 1975. Simulation of the physical subsystem of a mountain stream ecosystem by digital computer. PhD. Thesis, Utah State University, Logan, Utah.

U.S. Army Corps of Engineers. 1956. Snow hydrology, summary report of snow investigations. North Pacific Division, Portland, Oregon. 437 p.

U.S. Army Corps of Engineers. 1960. Runoff from snowmelt. Engineering and Design Manual 1110-2-1406. 75 p.

U.S. Department of Commerce, Environmental Science Services Administration, Weather Bureau. 1961 through 1970. Climatological data; Washington.

APPENDIX

Listing of Utah State University Watershed Simulation Model Computer Program

```
C *** MAIN PROGRAM - UTAH STATE UNIVERSITY WATERSHED SIMULATION MODEL
      COMMON/BLK1/PRCP(12,31),TEMP(12,31),STRM(12,31),COMP(12,31)
     2/BLK2/CP(12),RAD(12),MON(12),SUMN(12),SUMY(8),KW,KR,AREA,TCF
     3/BLK3/ETF,CPF,SI,SS,SFC,WILT,FD,FC,SMR,AVD,SNGM,TGW,TSW,TFWSN,
     4DK,PK,TRAIN,TMELT,TSNOW,SIO,SNIC,SMOIC,RSW,KTRL,KNTR,SMM,WHM,AVSM,
     5DDJ,NYR,MYR,NSW,IYR,KK,ENIC,IMJ,SMIC,CT,TX,IWS
C **  INITIALISE
C     KR=READER CONTROL    KW=WRITE CONTROL
      KR=6
      KW=6
      MYR=0
      NYR=0
    1 M=0
      MO=0
      TRAIN=38.
      TSNOW=36.
      DO 25 I=1,6
   25 SUMY(I)=0.
      DO 200 I=1,2
  200 WRITE(KW,23)
   23 FORMAT(1H1,21HMONTHLY WATER BALANCE)
C **  INPUT AND CALCULATE MONTHLY AND ANNUAL WATER BALANCE
      PAUSE 1
C *   READ 1ST YEAR NO AND WATERSHED NO
      IYR=IYR-1961
      IF(NYR.GT.1)GOTO 110
      READ(KR,10)IYR,IWS
   10 FORMAT(2I1)
  110 IMJ=12
      IF(IYR.EQ.9)IMJ=9
C *   READ DAILY CLIMATOLOGICAL AND HYDROLOGIC DATA FOR IYR TH YEAR
      CALL DREAD(IYR,IWS)
      IYR=IYR+1962
C     MONTHLY LOOP
      DO 22 M=1,IMJ
      MO=MO+1
      IF(MO.EQ.13)MO=1
      DO 17 J=1,6
   17 SUMN(J)=0.
      MDAY=MON(M)
C     DAILY LOOP
      DO 20 I=1,MDAY
      SUMN(1)=SUMN(1)+PRCP(M,I)
      SUMN(2)=SUMN(2)+STRM(M,I)
      SUMN(3)=SUMN(3)+TEMP(M,I)
      PPT=PRCP(M,I)
C     SEPARATE RAIN AND SNOW
      TEMR=TEMP(M,I)
      IF(TEMR-TSNOW)38,38,40
   38 SNOW=PPT
      PPT=0.0
      GO TO 49
   40 IF(TEMR-TRAIN)42,42,44
   42 SNOW=PRCP(M,I)*(TRAIN-TEMR)/(TRAIN-TSNOW)
      PPT=PPT-SNOW
      GO TO 49
```



```
C     KNTR=2 DAILY OUTPUT AND ALL GRAPHS
C     KTRL=1 SINGLE YEAR RUN MANUAL VERIFICATION
C     KTRL=2 CONTINUOUS RUN MANUAL VERIFICATION
C     KTRL=3 PARAMETER OPTIMIZATION
      GO TO (2,3,4),KTRL
C *   SINGLE YEAR RUN, MANUAL VERIFICATION
    2 CALL HYDRGY
      IF(KNTR.EQ.0) GO TO 50
      CALL GRAPH
      GO TO  50
C *   CONTINUOUS RUN, MANUAL VERIFICATION
    3 CALL HYDRGY
      MYR=MYR+1
      IF(KNTR.EQ.0) GO TO 136
      CALL GRAPH
  136 IF(NYR-MYR)150,150,1
C *   PARAMETER OPTIMIZATION
    4 CALL HYDRGY
      KK=1
      CALL OPTVER
      MYR=MYR+1
      IF(KNTR.EQ.0) GO TO 137
      CALL GRAPH
  137 IF(NYR-MYR)150,150,1
C **  OPTION OF NEW RUN WITHOUT READING DAILY DATA AND WATERSHED
C     CHARACTERISTIC DATA AGAIN
  150 WRITE(2,233)
  233 FORMAT(18HTYPE 1 FOR NEW RUN)
      READ(2,10)ISTOP
      NYR=0
      IF(ISTOP.EQ.1)GOTO 51
      STOP
      END
```

```
   44  SNOW=0.
    49 SUMN(4)=SUMN(4)+PPT
       SUMN(5)=SUMN(5)+SNOW
    20 CONTINUE
       SUMN(3)=SUMN(3)/FLOAT(MDAY)
       PLOSS=SUMN(1)-SUMN(2)
       IF(SUMN(5).LE.0.)SUMN(5)=0.
       WRITE(KW,21) MO,SUMN(1),SUMN(2),SUMN(3),PLOSS,SUMN(4),SUMN(5)
    21 FORMAT(1X,I4,1X,3HPPT,F5.2,1X,3HSTM,1X,F5.2,1X,3HTEM,1X,F5.2,1X,4H
      1LOSS,1X,F5.2,1X,2HRN,1X,F5.2,1X,2HSN,1X,F5.2)
       SUMY(1)=SUMY(1)+SUMN(1)
       SUMY(2)=SUMY(2)+SUMN(2)
       SUMY(3)=SUMY(3)+SUMN(3)/FLOAT(IMJ)
       SUMY(4)=SUMY(4)+SUMN(4)
    22 SUMY(5)=SUMY(5)+SUMN(5)
       YLOSS=SUMY(1)-SUMY(2)
       WRITE(KW,24)
    24 FORMAT(1X,20HYEARLY WATER BALANCE)
       WRITE(KW,21) IYR,SUMY(1),SUMY(2),SUMY(3),YLOSS,SUMY(4),SUMY(5)
       IF(NYR.GT.0) GO TO 57
       WRITE(KW,5)
     5 FORMAT(1X,29HWATERSHED CHARACTERISTIC DATA)
C *    READ WATERSHED CHARACTERISTIC DATA
C 1    AREA
       READ(KR,7)AREA
       WRITE(KW,7)AREA
     7 FORMAT(2F10.2)
C 2    MONTHLY RADIATION INDEX
       READ(KR,8)(RAD(M),M=10,12),(RAD(M),M=1,9)
  8    FORMAT(4X,12F4.2)
C 3    MONTHLY EVAPORATION INDEX
       READ(KR,9)(CP(M),M=1,12)
  9    FORMAT(3X,12F6.3)
       WRITE(KW,6)(CP(M),M=1,12),(RAD(M),M=1,12)
     6 FORMAT(2X,2HCP,1X,12F6.5/2X,3HRAD,1X,12F5.2)
C *    READ MODEL PARAMETERS
       GOTO 50
   51  PAUSE 10101
    50 READ(KR, 39) SIO,SNIC,SMOIC,AVSM,KNTR,KTRL,NYR
       WRITE(KW,39) SIO,SNIC,SMOIC,AVSM,KNTR,KTRL,NYR
    39 FORMAT(4F10.4,3I10)
       READ(KR,37)ETF,SI,AVD,SMR,FO,FC,TSW
       WRITE(KR,37)ETF,SI,AVD,SMR,FO,FC,TSW
       READ(KR, 37) CPF,WHM,BK,SNGM,TFWSN,TMELT
       WRITE(KW,37) CPF,WHM,BK,SNGM,TFWSN,TMELT
       READ(KR, 37) SS,SFC,WILT,GK,TGW,SMM,TRAIN,TSNOW
       WRITE(KW,37) SS,SFC,WILT,GK,TGW,SMM,TRAIN,TSNOW
    37 FORMAT(8F10.4)
    57 WRITE(KW,47)
    47 FORMAT(1X,29HHYDROLOGIC DATA--MODEL OUTPUT)
C      INITIALISE
       ENIC=AVSM
       SMIC=SMOIC
C **   SELECT OPTIONS BY USING CONTROL PARAMETERS KNTR AND KTRL
       KK=0
       MYR=0
C      KNTR=0 OUTPUT ONLY MONTHLY SUMMARY
C      KNTR=1 DAILY OUTPUT AND COMPUTE HYDROGRAPH
```



```
       SUBROUTINE DREAD(IY,IWS)
C *** TO TRANSFER WENATCHEE DATA FROM MAG TAPE TO MAIN SIM PROGRAM
       COMMON/BLK1/PRCP(12,31),TEMP(12,31),STRM(12,31),COMP(12,31)
      2/BLK2/CP(12),RAD(12),MDN(12),SUMN(12),SUMY(8),KW,KR,AREA,TCF
      3/BLK3/ETF,CPF,SI,SS,SFC,WILT,FO,FC,SMR,AVD,SNGM,TGW,TSW,TFWSN,
      4GK,BK,TRAIN,TMELT,TSNOW,SIO,SNIC,SMOIC,RSW,KTRL,KNTR,SMM,WHM,AVSM,
      5OBJ,NYR,MYR,NSW,IYR,KK,ENIC,IMJ,SMIC,CT,TX
       DOUBLE PRECISION NAME
       DATA NAME/6HWENDAT/
  500  FORMAT(3I2)
  513  FORMAT(I2,3(F4.2,F5.1,F6.2))
  514  FORMAT(18HINCORRECT ID  GEN=,I2,7H  READ=,I2)
C **   INITIALISE
       IF(MYR.NE.0)GOTO 5
       CALL QMON(22,13)
       CALL QMON(21,NAME,1,13)
C **   LOCATE REQUIRED YEAR KY
  5    READ(13,500)KY,KM,MDN(1)
       IF(KY-IY)15,25,10
  10   CALL QMON(12)
       GOTO 5
  15   IMI=12
  18   DO 20 IM=1,IMI
       IF(IM.NE.1)READ(13,500)KY,KM,MDN(IM)
       KD2=MDN(IM)
       DO 20 ID=1,KD2
  20   READ(13,513)KSKIP
       GOTO 5
C **   READ YEAR KY OF DATA
  25   IF(KM.EQ.4)GOTO 28
       IMI=3
       GOTO 18
  28   DO 30 IM=1,IMJ
       IF(IM.NE.1)READ(13,500)KY,KM,MDN(IM)
       KD2=MDN(IM)
       DO 30 ID=1,KD2
       GOTO(35,40,45),IWS
  35   READ(13,513)JD,PRCP(IM,ID),TEMP(IM,ID),STRM(IM,ID)
       GOTO 50
  40   READ(13,513)JD,A,B,C,PRCP(IM,ID),TEMP(IM,ID),STRM(IM,ID)
       GOTO 50
  45   READ(13,513)JD,A,B,C,A,B,C,PRCP(IM,ID),TEMP(IM,ID),STRM(IM,ID)
  50   IF(JD.NE.ID)WRITE(1,514)ID,JD
       STRM(IM,ID)=STRM(IM,ID)/1000.0
  30   CONTINUE
       RETURN
       END
```

```
      SUBROUTINE HYDRGY
C *** FOREST WATERSHED HYDROLOGIC SYSTEM SIMULATION
      COMMON/BLK1/PRCP(12,31),TEMP(12,31),STRM(12,31),COMP(12,31)
     2/BLK2/CP(12),RAD(12),MDN(12),SUMN(12),SUMY(8),KW,KR,AREA,TCF
     3/BLK3/ETF,CPF,SI,SS,SFC,WILT,FO,FC,SMR,AVD,SNGM,TGW,TSW,TFWSN,
     4QK,QK,TRAIN,TMELT,TSNOW,SIO,SNIC,SMOIC,RSW,KTRL,KNTR,SMM,WHM,AVSM,
     5OBJ,NYR,MYR,NSW,IYR,KK,ENIC,IMJ,SMIC,CT,TX,IWS
C **  INITIALISE
      MO=9
      IF(MYR.EQ.8)GO TO  9
      IF(NYR.GT.0)GO TO 51
    9 RSW=0.
      CPR=0.
      SDAY=0.
      FT=FC
      T1=60.
      T2=60.
      FWSN=0.
      SNRF=0.
   51 DO 5 I=1,8
    5 SUMY(I)=0.
      AVSM=ENIC
      SMOIC=SMIC
      DO 120 M=1,IMJ
      EPM=CP(M)*ETF
      SNF=SMR*RAD(M)
C     MONTHLY LOOP
      DO 15 J=1,12
   15 SUMN(J)=0.
      MDAY=MDN(M)
C     DAILY LOOP
      DO 100 I=1,MDAY
      RAIN=0.
      QSW=0.
      GWR=0.
      Z1=0.
      SRO=0.
      CHPF=0.
      PPT=PRCP(M,I)
C **  SEPARATE RAIN AND SNOW
      TEMR=TEMP(M,I)
      IF(TEMR-TSNOW)38,38,40
   38 SNOW=PRCP(M,I)
      PPT=0.0
      GO TO 49
   40 IF(TEMR-TRAIN)42,42,44
   42 SNOW=PRCP(M,I)*(TRAIN-TEMR)/(TRAIN-TSNOW)
      PPT=PPT-SNOW
      GO TO 49
   44 SNOW=0.0
   49 COMP(M,I)=0.0
C **  RAIN ON CHANNEL
      CHPPT=PPT*CPF+CPR
      PPT=PPT*(1.-CPF)
      CPR=CHPPT*EXP(-TSW)
      CHPF=CHPPT-CPR
```



```
  156 IF(Y-SWH-WHC)157,157,158
  157 SNRF=((Y-WHC)**2)/(2.0*SWH)
      SNIC=SNIC-((Y-WHC)**2)/(2.0*SWH)
      GOTO 36
  158 SNRF=FWSN-WHC
      SNIC=SNIC-SNRF
   36 IF(SNIC.GT.0.)GOTO 35
      SNRF=SNICB+RAIN+RSW
      RAIN=0.
      RSW=0.
      FWSN=0.
      SNIC=0.
      GO TO141
   35 WHCE=SNIC*0.05
      SNRF=SNRF+(WHC-WHCE)
      SNIC=SNIC-(WHC-WHCE)
      FWSN=WHCE
  138 IF(TEQ.GE.32.) GO TO141
      FWSN=FWSN*EXP(-TFWSN*(32.-TEQ))
  139 IF(FWSN.LE.0.0)FWSN=0.
      GO TO141
  140 SNRF=0.
C **  TOTAL AVAILABLE SURFACE WATER
  141 RAIN=RAIN+SNRF+RSW
C **  DETERMINE INFILTRATION RATE
   60 IF(RAIN-FC) 64,64,62
   62 FT=FC+FO*(SS-SMOIC)/SS
      SFW=RAIN-FT
      IF(SFW)64,64,66
C **  SOIL MOISTURE STORAGE
   64 SMOIC=SMOIC+RAIN
      RSW=0.
      GO TO 72
   66 SMOIC=SMOIC+FT
C **  SURFACE RUNOFF
      RSW=SFW*EXP(-TSW)
      SRO=SFW-RSW
      SUMN(2)=SUMN(2)+SRO
C **  EVAPOTRANSPIRATION
   72 EVP=TEMP*EPM/FLOAT(MDAY)
      SUMN(3)=SUMN(3)+EVP
      SUMN(4)=SUMN(4)+EVP
      IF(EVP.LT.SIO)GOTO 74
      EVP=EVP-SIO
      SIO=0.
      IF(EVP.LT.SNIC)GOTO 76
      EVP=EVP-SNIC
      SNIC=0.
      IF(SMOIC.GT.WILT)GOTO 92
      EEVP=EVP*SMOIC/WILT
      SMOIC=SMOIC-EEVP
      SUMN(4)=SUMN(4)+EEVP-EVP
      GO TO 70
   74 SIO=SIO-EVP
      GO TO 70
   76 SNIC=SNIC-EVP
      GO TO 70
   92 SMOIC=SMOIC-EVP
```

```
C **  INTERCEPTION
      IF(PPT+SNOW)55,55,11
   11 DSI=SI-SIO
      IF(PPT-DSI)52,53,54
   52 SIO=SIO+PPT
      SUMN(1)=SUMN(1)+PPT
      RAIN=0.
      GO TO 55
   53 SIO=SI
      SUMN(1)=SUMN(1)+SI
      RAIN=0.
      GO TO 55
   54 SIO=SI
      SUMN(1)=SUMN(1)+DSI
      RAIN=PPT-DSI
C **  SNOW ACCUMULATION AND MELT
   55 IF(SNIC.LT.SNGM)GOTO 1000
      SNIC=SNIC-SNGM
      SMOIC=SMOIC+SNGM
      GOTO 1010
 1000 SMOIC=SMOIC+SNIC
      SNIC=0.
 1010 TEQ=0.1*T1+0.3*T2+0.6*TEMR
      T1=T2
      T2=TEMR
      IF(SNOW.GT.0.)GO TO 31
      IF(SNIC.LE.0.)GO TO140
   31 SNIC=SNIC+SNOW
      SNICB=SNIC
      WHC=SNIC*0.35
      SDAY=SDAY+1.0
      IF(SNOW.NE.0.) SDAY=0.
      ALBD=0.40+(1.+EXP(-0.2*SDAY))
      IF(RAIN.NE.0.)ALBD=0.4
C *   SNOWMELT AMOUNT
      SMAM=SNF*(TEQ-TMELT)*(1.-ALBD)+(TEMR-32.0 )*1.0*RAIN/144.
      IF(SMAM.LE.0.) SMAM=0.
      IF(SMAM.LE.SNIC)GOTO 28
      SMAM=SNIC
      SNIC=0.
      SNRF=SMAM
      GO TO141
C *   FREE WATER IN SNOW PACK
   28 FWSN=FWSN+SMAM+RAIN+RSW
      SNIC=SNIC+RAIN+RSW
      RSW=0.
      RAIN=0.
      SWH=WHM*WHC
      Y=2.0*SWH*FWSN
      IF(Y.LT.0.00001)GOTO 159
      Y=SQRT(Y)
      PA=Y/SWH
      IF(PA.LE.1.0)GOTO 155
      Y=FWSN+SWH/2.0
  155 IF(Y.GT.WHC)GOTO 156
C *   RUNOFF FROM SNOW
  159 SNRF=0.
      GO TO138
```



```
C **  INTERFLOW
   70 IF(SMOIC-SFC)150,84,152
  150 GSW=SFC-SMOIC
      ZI=GSW*SMM
      SMOIC=SMOIC+ZI
      GOTO 154
  152 GSW=SMOIC-SFC
      GSWI=GSW*EXP(-TGW)
      OSW=GSW-GSWI
      SMOIC=SMOIC-OSW
      GWR=(1.-BK*(1.-GSW/SS))*OSW
      OSW=OSW-GWR
  154 SUMN(5)=SUMN(5)+OSW
      SUMN(11)=SUMN(11)+GWR-ZI
C **  BASEFLOW FROM INTERMEDIATE ZONE IN THE ZONE OF AERATION
   84 AVSM=(AVSM*(AVD-1.)+SMOIC)/AVD
      BF=BK*AVSM
      SUMN(6)=SUMN(6)+BF
      RUNOFF=(SRO+OSW+BF+CHPF)
C **  MONTHLY SUMMARY
      SUMN(7)=SUMN(7)+RUNOFF
      ERR=STRM(M,I)-RUNOFF
      COMP(M,I)=COMP(M,I)+RUNOFF
      SUMN(8)=SUMN(8)+ERR
C *   CALCULATE OBJECTIVE FUNCTION
      SUMN(9)=SUMN(9)+ABS(ERR)
      SUMN(10)=SUMN(10)+ERR*ERR
  100 CONTINUE
C **  YEARLY SUMMARY
      SUMY(1)=SUMY(1)+SUMN(3)
      SUMY(2)=SUMY(2)+SUMN(7)
      SUMY(3)=SUMY(3)+SUMN(8)
      SUMY(4)=SUMY(4)+SUMN(9)
      SUMY(8)=SUMY(8)+(SUMN(6)-SUMN(11))
      SUMY(6)=SUMY(6)+SUMN(1)
      SUMY(7)=SUMY(7)+SUMN(4)
      IF(KK.EQ.1)GO TO 120
      MO=MO+1
      IF(MO.EQ.13)MO=1
      IF(MO.EQ. 1)GO TO 103
      GO TO 105
C **  OUTPUT SUMMARY REPORTS
  103 WRITE(KW,121)MO,IYR
  121 FORMAT(1X,I2,1H-,I4)
      GO TO 106
  105 WRITE(KW,101)MO
  101 FORMAT(1X,I2)
  106 WRITE(KW,102) SUMN(1),SNIC,SMOIC,SUMN(11),SUMN(3),SUMN(4)
  102 FORMAT(1X,2HSI,F6.2,2X,2HSN,F6.2,2X,2HSM,F6.2,2X,2HGW,F6.2,2X,
     12HEP,F6.2,2X,2HAV,F6.2,5X,2X,F6.2)
      WRITE(KW,104) SUMN(2),SUMN(5),SUMN(6),SUMN(7),SUMN(8),SUMN(9),
     1SUMN(10)
  104 FORMAT(1X,2HSR,F6.2,2X,2HIF,F6.2,2X,2HBF,F6.2,2X,2HRF,F6.2,2X,
     12HER,F6.2,2X,2HAE,F6.2,2X,2HVR,F10.2)
  120 CONTINUE
      OBJ=SUMY(4)
      IF(KK.EQ.1)GO TO 199
      WRITE(KW,122) SUMY(2),SUMY(3),SUMY(4),SUMY(8),SUMY(1),SUMY(6),
```

```
      2SUMY(7)
  198 FORMAT(1X,CHANNUAL PF,F6.2,2X,2HER,F6.2,2X,2HAE,F6.2,2X,3HGWR,
     1F9.4, 2X,2HPE,      F6.2,2X,2HSI,F6.2,2X,2HAV,F6.2///)
  199 RETURN
      END
```



```
      SUBROUTINE OPTVER
C *** PARAMETER OPTIMIZATION
      COMMON/BLK1/PRCP(12,31),TEMP(12,31),STRM(12,31),COMP(12,31)
     2/BLK2/CP(12),RAD(12),MDN(12),SUMN(12),SUMY(8),KW,KR,AREA,TCF
     3/BLK3/ETF,CPF,SI,SS,SFC,WILT,FO,FC,SMR,AVO,SNGM,TGW,TSW,TFWSN,
     4SK,RK,TRAIN,TMELT,TSNOW,SIO,SNIC,SMOIC,RSW,KTRL,KNTR,SMM,WHM,AVSM,
     5OBJ,NYR,MYR,NSW,IYR,KK,ENIC,IMJ,SMIC,CT,TX,IWS
      DIMENSION XIN(6,12),XMN(12),XPM(12),DF(12),OBI(12),PL(12),PH(12),
     1NL(12),PR(12)
C **  READ PATTERN SEARCH BOUNDS AND LEVELS
      IF(MYR.EQ.0)GO TO 299
      IF(NYR.GT.0)GO TO 310
  299 READ(KR,300)NPH,NPR
  300 FORMAT(2I10)
      DO 309 LL=1,NPR
  309 READ(KR,301)L,XIN(1,L),PL(L),PH(L),NL(L)
  301 FORMAT(I2,17X,3(F8.0,2X),I2)
  310 OBI(1)=OBJ
C **  INITIALIZE MINIMUM CONDITIONS
      PRMN=OBJ
      PHMN=OBJ
      DO314 L=1,NPR
      XMN(L)=XIN(1,L)
      XPM(L)=XIN(1,L)
      PR(L)=XIN(1,L)
  314 DF(L)=PH(L)-PL(L)
C *   TAKE NEW PAGE WRITE PH,PL, NL
      WRITE(KW,302)
  302 FORMAT(1H1///19X,3HPAR,8X,2HPH,8X,2HPL,8X,2HDF,8X,2HNL///)
      DO315 L=1,NPR
  315 WRITE(KW,303)L,PH(L),PL(L),DF(L),NL(L)
  303 FORMAT(15X,I7,3X,3F10.3,I7)
  304 FORMAT(1H1//20X,5HPHASE,I3,2X,5HPMIN=,F10.4)
  305 FORMAT(5X,10F7.3)
  306 FORMAT(///6X,13HIP  LV    PAR,10X,3HOSJ)
  307 FORMAT(5X,I3,2X,I3,F11.3,5F11.4)
  308 FORMAT(5X,I3,2H *,I3,F11.3,5F11.1)
C **  BEGIN PHASE LOOP
      DO390K=1,NPH
C *   TAKE NEW PAGE WRITE PHASE ONE INITIAL VECTOR
      WRITE(KW,304)K,PHMN
      WRITE(KW,305)(XIN(K,L),L=1,NPR)
      WRITE(KW,306)
C **  BEGIN PAR LOOP
      DO380  J=1,NPR
      NLO=NL(J)+1
      IF(NLO.LE.2)GO TO 380
C **  BEGIN INCR LOOP
      DO370 I=1,NLO
      IF(I.GT.1)GO TO 340
      XNL=NL(J)
      DS=DF(J)/XNL
  340 XI=(I-1)
      PR(J)=PL(J)+DS*XI
C *   OPERATE MODEL AND DETERMINE OBJECTIVE FUNCTION
  349 CALL PARSET(J,PR(J))
```

```
      SUBROUTINE PARSET(IP,PC)
C *** SET PARAMETERS TO BE OPTIMIZED
      COMMON/BLK1/PRCP(12,31),TEMP(12,31),STRM(12,31),COMP(12,31)
     2/BLK2/CF(12),RAD(12),MDN(12),SUMN(12),SUMY(8),KW,KR,AREA,TCF
     3/BLK3/ETF,CPF,SI,SS,SFC,WILT,FO,FC,SMR,AVD,SNGM,TGW,TSW,TFWSN,
     40K,BK,TRAIN,THELT,TSNOW,SIO,SNIC,SMOIC,RSW,KTRL,KNTR,SMM,WHM,AVSM,
     50BJ,NYR,MYR,NSW,IYR,KK,ENIC,IMJ,SMIC,CT,TX,IWS
      GOTO(1,2,3,4,5,6,7,8,9,10,11,12),IP
    1 BK=PC
      GOTO 99
    2 QK=PC
      GOTO 99
    3 SFC=PC
      GOTO 99
    4 TGW=PC
      GOTO 99
    5 SMR=PC
      GOTO 99
    6 AVD=PC
      GOTO 99
    7 WILT=PC
      GOTO 99
    8 THELT=PC
      GOTO 99
    9 WHM=PC
      GOTO 99
   10 FC=PC
      GOTO 99
   11 SS=PC
      GOTO 99
   12 FO=PC
   99 RETURN
      END
```



```
      CALL HYDRGY
      WRITE(KW,367)J,I,PR(J),OBJ
C *   IF NEW PAR. INITIALIZE LOCAL MIN
      IF(I.GT.1)GO TO 367
      PRMN=OBJ
      XMN(J)=PR(J)
C *   CHECK LOCAL AND PHASE MINS
      GO TO 351
  367 IF(OBJ-PRMN)350,351,351
  350 PRMN=OBJ
      XMN(J)=PR(J)
  351 IF(OBJ-PHMN)352,370,370
  352 PHMN=OBJ
      DO353 L=1,NPR
  353 XPM(L)=PR(L)
  370 CONTINUE
C *   RESET PR(J) TO FIXED LEVEL FOR NEXT PAR.
  372 PR(J)=XMN(J)
      CALL PARSET(J,PR(J))
      CALL HYDRGY
  380 CONTINUE
C **  SELECT BEST VECTOR FOR NEXT PHASE
      IF(PRMN-PHMN)384,386,386
  384 KFJ=K+1
      DO 385 L=1,NPR
      XIN(KFJ,L)=XMN(L)
      PR(L)=XMN(L)
  385 CALL PARSET(L,PR(L))
      GO TO 388
  386 KFJ=K+1
      DO 387 L=1,NPR
      XIN(KFJ,L)=XPM(L)
      PR(L)=XPM(L)
  387 CALL PARSET(L,PR(L))
  388 CALL HYDRGY
      OBI(K+1)=OBJ
  390 CONTINUE
C **  WRITE OUT INITIAL VECTOR TABLE
      NHP=NPH+1
      WRITE(KW,109)(OBI(L),L=1,NHP)
  109 FORMAT(1H1//27X,15HINITIAL VECTORS//10X,5HPHASE,7X,1H1,9X,1H2,9X,
     11H3,9X,1H4,9X,1H5//12X,3HOBJ,5F10.4/)
      WRITE(KW,110)
  110 FORMAT(12X,3HPAR/)
      NPT=NPH+1
      DO91 L=1,NPR
   91 WRITE(KW,111)L,(XIN(M,L),M=1,NPT)
  111 FORMAT(12X,I3,5F10.3)
      KK=0
      CALL HYDRGY
      KK=1
      RETURN
      END
```

```
      SUBROUTINE GRAPH
C *** SUBROUTINE TO PLOT COMPUTED AND OBSERVED CLIMATOLOGIC AND
      COMMON/BLK1/PRCP(12,31),TEMP(12,31),STRM(12,31),COMP(12,31)
C     2/BLK2/CP(12),RAD(12),MDN(12),SUMN(12),SUMY(8),KW,KR,AREA,TCF
C     3/BLK3/ETF,CPF,SI,SS,SFC,WILT,FD,FC,SMR,AVD,SNGM,TGW,TSW,TFWSN,
C     4QK,BK,TRAIN,TMELT,TSNOW,SIO,SNIC,SMOIC,RSW,KTRL,KNTR,SMM,WHM,AVSM,
C     5QBJ,NYR,MYR,NSW,IYR,KK,ENIC,IMJ,SMIC,CT,TX,IWS
      DATA JJ,XSCALE,YSCALE,XREF,YREF,XP,YN,XVAL,XN,YVAL,YP/0,1.,1.,0.,0
     1.,19.,0.,0.,0.,-9.,10./
      DATA ISP,ISLSW/1H ,1H//
      CALL PLTSET(XSCALE,YSCALE,XREF,YREF,XVAL,YVAL,XP,YP,XN,YN)
      CALL SRYSET
      IF(KNTR.EQ.1)GOTO 241
      JJ=0
C **  STREAMFLOW PLOTTING - OBSERVED
      DO 240 M=1,IMJ
      MDAY=MDN(M)
      CALL PENDN
      DO 235 I=1,MDAY
      JJ=JJ+1
      X=FLOAT(JJ)*(.05)
      YY=STRM(M,I)
      Y=ALOG10(YY)*3.0
      CALL PLOT(X,Y)
  235 CONTINUE
      CALL SYMBOL(1)
      CALL PENUP
  240 CONTINUE
      CALL STNDBY
      PAUSE 1
C     TAKE OUT OF RUN    CHANGE PEN COLOR
C **  STREAMFLOW PLOTTING - COMPUTED
  241 JJ=0
      DO 250 M=1,IMJ
      MDAY=MDN(M)
      CALL PENDN
      DO 245 I=1,MDAY
      JJ=JJ+1
      X=FLOAT(JJ)*(.05)
      Y=ALOG10(YY)*3.0
      CALL PLOT(X,Y)
  245 CONTINUE
      CALL SYMBOL(1)
      CALL PENUP
  250 CONTINUE
      IF(KNTR.EQ.1)CALL STNDBY
      IF(KNTR.EQ.1)RETURN
      X=0.
      Y=10.
      CALL INPLOT (X,Y)
      JJ=0
      YP=0.
      YVAL=0.
      YN=-12.
      CALL PLTSET(XSCALE,YSCALE,XREF,YREF,XVAL,YVAL,XP,YP,XN,YN)
      CALL SRYSET
```



```
      PAUSE 1
C **  PRECIP PLOTTING
      DO 230 M=1,IMJ
      MDAY=MDN(M)
      CALL PENDN
      DO 225 I=1,MDAY
      JJ=JJ+1
      X=FLOAT(JJ)*(.05)
      YY=PRCP(M,I)
      Y=-YY+1.27
      X=X-.05
      CALL INPLOT(X,Y)
      X=X+.05
      CALL INPLOT(X,Y)
  225 CONTINUE
      CALL SYMBOL(1)
  230 CONTINUE
      CALL PENUP
      X=0.
      Y=-9.
      CALL INPLOT(X,Y)
      JJ=0
      YN=-1.
      CALL PLTSET(XSCALE,YSCALE,XREF,YREF,XVAL,YVAL,XP,YP,XN,YN)
      CALL SRYSET
C **  TEMP PLOTTING
      DO 260 M=1,IMJ
      MDAY=MDN(M)
      CALL PENDN
      DO 255 I=1,MDAY
      JJ=JJ+1
      X=FLOAT(JJ)*.05
      YY=(TEMP(M,I)-32.)*5./9.
      Y=YY*.05
      X=X-.05
      CALL INPLOT(X,Y)
      X=X+.05
      CALL INPLOT(X,Y)
  255 CONTINUE
      CALL SYMBOL(1)
  260 CONTINUE
      CALL PENUP
      CALL INPLOT(X,Y)
      JJ=0
      YP=10.
      Y=0.
      YVAL=-9.
      RETURN
      END
```